Received: 17 February 2023 | Accepted: 2 July 2023

DOI: 10.1002/tpg2.20372

The Plant Genome

ORIGINAL ARTICLE

Special Section: Genomics of Abiotic Stress Tolerance and Crop Resilience to Climate Change

Integrative multi-omics analyses of date palm (*Phoenix dactylifera*) roots and leaves reveal how the halophyte land plant copes with sea water

Heike M. Mueller[1] | **Bastian L. Franzisky**[2] | **Maxim Messerer**[3] | **Baoguo Du**[4,5] | **Thomas Lux**[3] | **Philip J. White**[6] | **Sebastien Christian Carpentier**[7,8] | **Jana Barbro Winkler**[9] | **Joerg-Peter Schnitzler**[9] | **Hamed A. El-Serehy**[10] | **Khaled A. S. Al-Rasheid**[10] | **Naif Al-Harbi**[10] | **Saleh Alfarraj**[10] | **Jörg Kudla**[11] | **Jaakko Kangasjärvi**[12] | **Michael Reichelt**[13] | **Axel Mithöfer**[14] | **Klaus F. X. Mayer**[3] | **Heinz Rennenberg**[5] | **Peter Ache**[1] | **Rainer Hedrich**[1] | **Christoph-Martin Geilfus**[2]

[1]Institute for Molecular Plant Physiology and Biophysics, Biocenter, University Würzburg, Würzburg, Germany

[2]Department of Soil Science and Plant Nutrition, Hochschule Geisenheim University, Geisenheim, Germany

[3]Plant Genome and Systems Biology, Helmholtz Center Munich, Neuherberg, Germany

[4]College of Life Science and Biotechnology, Mianyang Normal University, Mianyang, China

[5]Chair of Tree Physiology, Institute of Forest Sciences, Albert-Ludwigs-Universität Freiburg, Freiburg, Germany

[6]The James Hutton Institute, Invergowrie, Scotland

[7]Facility for SYstems BIOlogy based MAss Spectrometry, SYBIOMA, Proteomics Core Facility, KU Leuven, Leuven, Belgium

[8]Division of Crop Biotechnics, Laboratory of Tropical Crop Improvement, KU Leuven, Leuven, Belgium

[9]Research Unit Environmental Simulation (EUS), Institute of Biochemical Plant Pathology, Helmholtz Center Munich, Neuherberg, Germany

[10]Zoology Department, College of Science, King Saud University, Riyadh, Saudi Arabia

[11]Institut für Biologie und Biotechnologie der Pflanzen, Westfälische Wilhelms-Universität Münster, Münster, Germany

[12]Faculty of Biological and Environmental Sciences, University of Helsinki, Helsinki, Finland

[13]Department of Biochemistry, Max Planck Institute for Chemical Ecology, Jena, Germany

[14]Research Group Plant Defense Physiology, Max Planck Institute for Chemical Ecology, Jena, Germany

Correspondence
Bastian L. Franzisky, Department of Soil Science and Plant Nutrition, Hochschule Geisenheim University, 65366 Geisenheim, Germany.
Email: bastianleander.franzisky@hs-gm.de

Maxim Messerer, Plant Genome and Systems Biology, Helmholtz Center Munich, 85764 Neuherberg, Germany.

Abstract

Date palm (*Phoenix dactylifera* L.) is able to grow and complete its life cycle while being rooted in highly saline soils. Which of the many well-known salt-tolerance strategies are combined to fine-tune this remarkable resilience is unknown. The precise location, whether in the shoot or the root, where these strategies are employed remains uncertain, leaving us unaware of how the various known salt-tolerance

Abbreviations: AO, aldehyde oxidase; GO, gene ontology; GSH, glutathione; JA, jasmonic acid; JA-Ile, jasmonoyl isoleucine; NCED, 9-*cis*-epoxycarotenoid dioxygenase; Pd, *Phoenix dactylifera*; ROS, reactive oxygen species; SA, salicylic acid; SOS, salt overly sensitive.

Email:
maxim.messerer@helmholtz-muenchen.de

Heike M. Mueller, Bastian L. Franzisky, Maxim Messerer, and Baoguo Du contributed equally.

Assigned to Associate Editor Rupesh Deshmukh.

[Correction added on August 17, 2023, after first online publication: author Peter Ache is removed as corresponding author.]

Funding information
King Saud University; German Research Foundation (German: Deutsche Forschungsgemeinschaft), Grant/Award Number: (471624304;GZ: GE 3111/5-1)

mechanisms are integrated to fine-tune this remarkable resilience. To address this shortcoming, we exposed date palm to a salt stress dose equivalent to seawater for up to 4 weeks and applied integrative multi-omics analyses followed by targeted metabolomics, hormone, and ion analyses. Integration of proteomic into transcriptomic data allowed a view beyond simple correlation, revealing a remarkably high degree of convergence between gene expression and protein abundance. This sheds a clear light on the acclimatization mechanisms employed, which depend on reprogramming of protein biosynthesis. For growth in highly saline habitats, date palm effectively combines various salt-tolerance mechanisms found in both halophytes and glycophytes: "avoidance" by efficient sodium and chloride exclusion at the roots, and "acclimation" by osmotic adjustment, reactive oxygen species scavenging in leaves, and remodeling of the ribosome-associated proteome in salt-exposed root cells. Combined efficiently as in *P. dactylifera* L., these sets of mechanisms seem to explain the palm's excellent salt stress tolerance.

1 | INTRODUCTION

The halophytic date palm (*Phoenix dactylifera* L.) is one of the most important crops in the semi- to hyperarid Arabian Peninsula. This is because of its tolerance to adverse environmental conditions such as heat, drought, and salt stress (Al-Bahrany & Al-Khayri, 2012; Arab et al., 2016; Du et al., 2021, 2021, 2023). However, there is limited knowledge regarding which of the well-known strategies for surviving salinity are employed by date palms, and nothing is known about whether these strategies are active in the roots, the shoots, or both. Excessive salt concentrations have various effects on plants. In the early (first) phase of exposure (days to weeks), plants face primarily osmotic stress. The "second" phase (weeks to month) is characterized by ionic stress, that is, the accumulation of salt ions such as sodium (Na^+) and chloride (Cl^-) in cells (Munns & Tester, 2008). To cope with the osmotic stress, glycophytic and halophytic plants may accumulate osmotically active compounds (Munns & Tester, 2008) such as amino acids and nonreducing sugars to lower the osmotic potential of the cell (Chen & Murata, 2002; Yaish, 2015). To avoid ion toxicities, either the uptakes of Na^+ and Cl^- are restricted or these ions are sequestered in cells, vacuoles or tissues that are less relevant to growth and photosynthesis (Blumwald et al., 2000; Li et al., 2017; Munns et al., 2016). Moreover, for protecting photosynthetically active cells, potassium (K^+) retention is important. Maintaining a high cytosolic K^+:Na^+ ratio is one of the key features of halophytes (Karimi et al., 2021; Munns & Tester, 2008; Rubio et al., 2020). In addition, stomatal regulation and abscisic acid (ABA) signaling play an important role in adjusting water consumption and mass flow-driven uptake of salt (Geilfus & Mühling, 2012; Karimi et al., 2021; Müller et al., 2017).

Due to global warming, sea level rises, leading to intensified saltwater intrusion in coastal groundwater aquifers. As a result, crops are more and more affected by salinity (i.e., brackish water in the underground) (Kaushal et al., 2018; Lassiter, 2021). In other words, saline water is increasingly entering the pedosphere, affecting the biosphere in these regions. Especially in irrigated drylands in arid and semi-arid regions that are already salt-affected, saltwater intrusion in sweet water aquifers makes the problem worse (Okur & Örçen, 2020). In this light, it is surprising that it is not yet understood which of the commonly known mechanisms for salt stress adaptation the date palm utilizes to grow while being exposed to seawater. Notably, this land plant has the capacity to complete its lifecycle while being confronted with sea water. A few authors have reported that the salt tolerance of date palm is based primarily on the ability to limit Na^+ uptake (Alhammadi & Edward, 2009; Bhat et al., 2013). However, we suspect that many more adjustments to plant physiology are necessary (Munns & Millar, 2023) that are based on extensive transcriptional, translational, and hormonal reprogramming.

To comprehend these adjustments, we exposed the date palm cultivar Khalas to salt stress and performed transcriptomic and proteomic analyses of roots and leaves. Usually, proteomic and transcriptomic data show poor convergence, suggesting manifold posttranslational changes. However, our approach of data integration achieved a degree of convergence that is usually unattained in plant sciences. This allows us to derive conclusions about the salt stress responses of date palm with a very small probability of error. Shared features between mRNAs and proteins were expressed as functional networks displaying metabolic processes that are responsive to salt stress. Validation by targeted-metabolomics, hormone profiling and tissue-specific ion- and gene-analysis confirmed

the responsiveness of these processes. With this integrative multi-omics approach in combination with follow-up testing, we gain new insights and draw novel conclusions on the salt tolerance of date palm: It is based on the combined ability to (i) express transporters that facilitate both the exclusion of Na^+ and Cl^- ions from roots and restrict their accumulation in leaves, (ii) mitigate oxidative stress, and (iii) adjust osmotically to extreme salt loads by the accumulation of amino acids.

Core Ideas

- Date palm is able to grow in extreme saline habitats by effectively orchestrating different tolerance strategies.
- Uptake of salt ions is significantly reduced by adjusting the root transportome, avoiding ion tissue toxicity.
- For osmotic adjustment, root and leaf cells predominantly accumulate amino acids rather than sugars.
- Oxidative damage is mitigated by boosting the antioxidative machinery in photosynthetically active tissue.
- Remodeling of the ribosome-associated proteome occurs in salt-exposed root cells.

2 | MATERIALS AND METHODS

2.1 | Plant material and growth conditions

Seedlings of micro-propagated *P. dactylifera*, cultivar Khalas, of about 2 years old were purchased from Date Palm Developments Ltd. Seedlings were planted in 5-L pots filled with 70% quartz gravel (3–5 mm diameter, Quarzwerke GmbH) and covered by 4 cm soil substrate (Floragard Vertriebs-GmbH).

2.1.1 | Greenhouse experiment

Plants were grown under 16:8 h, light:dark at 35 ± 2°C and 50% ± 5% relative humidity, 200 µmol photons m^{-2} s^{-1} at shoot height. To allow the plants to acclimate to the salt treatment, the NaCl concentration in the irrigation water was gradually increased from 100 to 200, 400 and 600 mM every second day. Plants were then watered with 600 mM NaCl solution every second day over 6 weeks, whereas controls received tap water. Roots of about 40 cm length were harvested and divided into five segments (R1 = most upper segment, R5 = root tip). Three different pinnae from one palm branch of each plant were harvested (P1–P3).

2.1.2 | Phytotron experiment

Plants were grown in walk-in phytotrons at the Research Unit of Environmental Simulation (EUS; Helmholtz Center Munich) to simulate climatic conditions of the date palm's natural habitat (14:10 h, light:dark; 35:18°C; approx. 30%:70% humidity, 600 µmol photons m^{-2} s^{-1} at shoot height) as described elsewhere (Du et al., 2018). Each plant was automatically irrigated by 50 mL of tap water every 4 h. After 2 weeks of acclimation, salt treatment started by gradually increasing NaCl concentrations in the irrigating water from 100 to 200, to 400, and to 600 mM every second day. The youngest fully expanded leaf and the whole root of 10 plants from each treatment were harvested for analysis of ions, elements, and metabolites at the day the salt concentration reached 600 mM (here referred to as day 0), on the 7th day, and on the 28th day of the 600 mM stress treatment. Samples from day 28 were additionally subjected to transcriptomic and proteomic analyses.

Plant materials of both experiments (total leaves, single pinnae, whole roots, or root segments) were cut into small pieces, homogenized in liquid nitrogen and stored at −80°C until further analyses.

2.2 | RNA extraction, cDNA synthesis, and qPCR

RNA isolation, cDNA synthesis, and qPCR were done as described previously (Paoletti et al., 2021). Transcript numbers were calculated for individual PCR products using standard curves and normalized to 10,000 transcripts of the housekeeping gene, that is, the growth elongation factor *P. dactylifera* EF1α (Patankar et al., 2016). The primers used are listed in Table S1f.

2.3 | Transcriptome analysis

RNA library preparation and sequencing were done at the Biomedicum Functional Genomics Unit (FuGU), for details see the Supporting Information section (Supplemental Material S1). The quality of the raw RNAseq reads was analyzed with FastQC (http://www.bioinformatics.babraham.ac.uk/projects/fastqc). The trimming step was performed with Trimmomatic (Bolger et al., 2014) using the parameters "ILLUMINACLIP:Illumina_PE_adapters.fasta:2:30:10:8:true LEADING:3 TRAILING:3 SLIDINGWINDOW:4:20 MINLEN:60." The reads were mapped to a

Trinity de novo assembly (Haas et al., 2013) using Kallisto (Bray et al., 2016). Details on assembly, construction and transcript annotations are given in the Supporting Information section. Differentially expressed genes were calculated using "EdgeR" (Robinson et al., 2010), for details see Supporting Information section. Filtering for low read counts resulted in 51,466 transcripts. RNAseq data were submitted to EMBL-EBI-Annotare (https://www.ebi.ac.uk/fg/annotare) under the ArrayExpress accession number E-MTAB-11 001.

2.4 | Proteome analysis and computational integration in transcriptomic data

Protein extractions were performed following the phenol-extraction/ammonium-acetate precipitation protocol described previously (Buts et al., 2014; Carpentier et al., 2005). In brief, after extraction, 20 µg of protein were digested with trypsin (Trypsin Protease, MS Grade Thermo Scientific) and purified by Pierce C18 Spin Columns (Thermo Scientific). The digested samples (0.5 µg/5 µL) were separated in an Ultimate 3000 (Thermo Scientific) UPLC system and then analyzed in an Orbitrap ELITE mass spectrometer (Thermo Scientific) equipped with an Acclaim PepMap100 pre-column (Thermo Scientific) and a C18 PepMap RSLC (Thermo Scientific) using a linear gradient of buffers A and B (0.300 µL min^{-1}). Buffer A was composed of pure water containing 0.1% formic acid; buffer B was composed of pure water containing 0.08% formic acid and 80% acetonitrile. The Orbitrap ELITE mass spectrometer (Thermo Scientific) was operated in positive ion mode with a nanospray voltage of 1.8 kV and a source temperature of 275°C. The instrument was operated in data-dependent acquisition mode with a survey MS scan at a resolution of 60,000 for the mass range of *m/z* 375–1500 for precursor ions, followed by MS/MS scans of the top 20 most intense peaks with +2, +3, +4, and + 5 charged ions. All data were acquired with Xcalibur 3.0.63.3 software (Thermo Scientific). For protein quantification, the software Progenesis (Nonlinear Dynamics) was applied using all peptides for quantification as described in Soares et al. (2018). We applied MASCOT version 2.2.06 (Matrix Science) against the assembled transcriptome (82,472 accessions) using the search parameters parent mass tolerance of 12 PPM, fragment tolerance of 0.2 Da, variable modification by oxidation M, Deamidation NQ, fixed modification by carbamidomethyl C, with up to 2 missed cleavages allowed for trypsin.

The proteomic data (4303 features, Table S2) were integrated into the transcriptomic data (51,466 features, Table S1). By searching the spectra against the mRNA database, transcript and protein abundances were linked to their gene (van Wesemael et al., 2018). Genes that were commonly up- or downregulated in both omics analyses were analyzed for gene ontology (GO) overrepresentation and visualized in cytoscape (Ma et al., 2021; Shannon et al., 2003). In this way, functional mRNA-protein networks were generated that reveal strong information on the complexity of the gene families and the biological processes underlying the date palm's ability to survive salinity.

2.5 | Na^+ and K^+ quantification by flame photometry (greenhouse experiment)

Na^+ and K^+ concentrations of the root and leave sections were measured using a flame photometer (PFP7, JENWAY) according to the manufacturer's instructions. For details see Supporting Information section.

2.6 | Element analysis (phytotron experiment)

The element concentrations of plant material were determined following acid digestion by inductively coupled plasma mass spectrometry essentially as described by White et al. (2012). For details of ion extraction see Supporting Information section.

2.7 | Biochemical analyses

Foliar H_2O_2 was extracted and assayed as described previously (Du et al., 2018; Velikova et al., 2000). In vitro glutathione (GSH) reductase (EC 1.8.1.7) and dehydroascorbate reductase (EC 1.8.5.1) activities in leaves were determined as described previously (Arab et al., 2016; Polle et al., 1990). Total and oxidized GSH, cysteine, and γ-glutamylcysteine were extracted and determined as described previously (Samuilov et al., 2016; Schupp & Rennenberg, 1988; Strohm et al., 1995). Total and reduced ascorbates were colometrically determinedas described previously (Du et al., 2018). For details on the quantification of total soluble protein and sugar, and determination of anions, see Supporting Information section. Relative abundances of water soluble low-molecular-weight metabolites in leaves were analyzed by GC–MS. Metabolites were extracted, derivatized, and separated as described previously (Du et al., 2018). Phytohormone extraction and related LC–MS analysis was performed as described previously (Davila-Lara et al., 2021; Vadassery et al., 2012).

2.8 | Statistical analysis

Biological replicates in the greenhouse experiment: ionome: $n = 5$; qPCR: $n = 3–5$, and the phytotron experiment: ionome: $n = 10$; phytohormones: $n = 8–10$; metabolome, antioxidants,

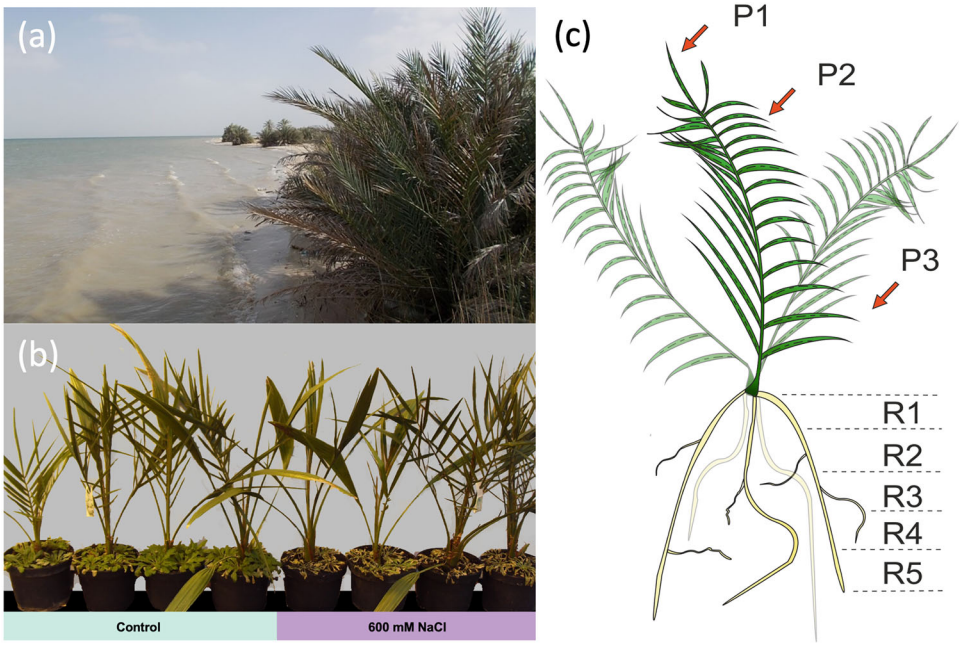

FIGURE 1 Salt tolerance of date palms (*Phoenix dactylifera* L.): (a) date palms at the Arabian Gulf with their roots in sea water, (b) date palms cv. Khalas in the greenhouse after 6 weeks of treatment with 600 mM NaCl. Note that the *Arabidopsis thaliana* plants in the pots died at 600 mM saline salt treatment, whereas the date palms remained unaffected, (c) five root segments (R1–R5) and three pinnae (P1–P3) were harvested for analyses.

soluble sugars: $n = 5$; proteome: $n = 4$; RNA-sequencing: $n = 3$. Data processing, analyses of variance, models, and post hoc tests (Tukey's) were performed using R (R Core Team, 2020). Data were analyzed using linear models and applying a significance threshold of $p \leq 0.05$. Data sets comprising unbalanced sample size due to missing values, namely, leaf qPCR and phytohormone data, were analyzed using Dunnett's all-pairs comparison test and mixed effect model with the individual phytotron growth chamber as random factor, respectively. Metabolite data were analyzed by *t*-tests. Data were plotted using "ggplot2" (Wickham, 2016).

3 | RESULTS AND DISCUSSION

3.1 | Transcript abundance of transporter for sodium export increases with Na^+ concentration in roots

Date palms are highly salt tolerant. That is, they are able to maintain the tissue concentration of Na^+ low (Al-Bahrany & Al-Khayri, 2012; Alhammadi & Edward, 2009; Bhat et al., 2013). This is certainly attributable to the activity of plasma membrane localized Na^+/proton (H^+) antiporter of the NHX (Na^+/H^+ exchanger)-family. However, it is still unknown whether these transporters are predominantly expressed in the shoot or already in the root. Additionally, it remains unclear for date palms whether chloride is also excluded, and if so, which transport proteins are accountable for this process. To shine a light on these questions, two consecutive experiments were conducted. The first experiment was performed in a greenhouse, where Na^+ uptake and transcript abundance of Na^+ transporters were studied in roots and leaves in high spatial resolution. In the second experiment, a phytotron was used to mimic the environmental conditions that prevail at the Arabian Peninsula. Samples of roots and leaves were subjected to an integrated analysis of the transcriptome and the proteome supplemented with tissue ion (Cl^-, Na^+, K^+, etc.), element, and metabolite measurements.

The fact that date palms grow directly at the coastline of the Arabian Gulf (Figure 1a) witnesses these desert plants' high tolerance to salinity. Although the roots reached into the seawater, plants looked healthy, almost without any visual injury to salt stress. To decipher the date palm's salt management strategy, we treated the highly salt tolerant cultivar Khalas (Yaish & Kumar, 2015) with 600 mM NaCl, mimicking the NaCl concentration of seawater, over 6 weeks (Figure 1b). To check the hypothesis that date palm excludes Na^+ efficiently, the concentration of Na^+ in roots and its distribution within the plant was analyzed. For this, the main root was divided into five segments, starting from the upper part directly below the shoot base (root segment 1; abbreviated R1) to the tip of the root (R5) (Figure 1c).

To monitor the allocation of Na^+ from the rooting medium to the leaves, single pinnae were sampled from the upper

TABLE 1 Transcript abundance of differentially expressed genes encoding date palm transporters involved in responses of roots and leaves to salt stress.

salt_root_K	name	Araport11_defline
-2.5	KAT2	potassium channel KAT1-like protein
-2.6	KCO6	Ca2+ activated outward rectifying K+ channel 6
-2.3	HAK5	high affinity K+ transporter 5
-2.8	HAK5	high affinity K+ transporter 5
-3.2	HAK5	high affinity K+ transporter 5
-3.2	HAK5	high affinity K+ transporter 5
-3.8	KUP1	potassium transporter 1
-5.0	KUP2	potassium transporter 2
-4.8	KUP2	potassium transporter 2
3.8	KUP2	potassium transporter 2
-2.3	KUP2	potassium transporter 2
-2.2	KUP6	K+ uptake permease 6
1.8	KUP7	K+ uptake permease 7
-1.9	KUP10	K+ uptake permease 10
-1.5	KUP11	K+ uptake permease 11
1.5	KUP11	K+ uptake permease 11
-13.8	AKT2/3	potassium transport 2/3
-22.2	AKT2/3	potassium transport 2/3
-2.6	KEA4	K+ efflux antiporter 4
2.4	SKOR	STELAR K+ outward rectifier
2.3	SKOR	STELAR K+ outward rectifier
-2.8	SKOR	STELAR K+ outward rectifier
-8.7	HKT1	Na+ transport, high-affinity K+ transporter 1
-19.3	HKT1	Na+ transport, high-affinity K+ transporter 1
-19.5	HKT1	Na+ transport, high-affinity K+ transporter 1
2.7	NHX2	sodium hydrogen exchanger 2
3.0	NHX2	sodium hydrogen exchanger 2
1.8	SOS1	sodium proton exchanger, putative (NHX7) (SOS1)
4.3	ALMT9	aluminum-activated malate transporter 9
2.1	SLAH1/4	SLAC1 homologue 1
-4.1	SLAH1/4	SLAC1 homologue 4
2.9	SLAH3	SLAC1 homologue 3
6.6	SLAH3	SLAC1 homologue 3
-2.5	STP3	Major facilitator superfamily protein
-3.4	STP5	Major facilitator superfamily protein
-2.7	STP5	Major facilitator superfamily protein

salt_shoot_K	name	Araport11_defline
6.3	AKT1	K+ transporter 1
6.7	AKT1	K+ transporter 1
2.8	KAT1	potassium channel KAT1
3.2	KAT2	potassium channel KAT1-like protein
-4.5	HAK5	high affinity K+ transporter 5
8.0	HAK5	high affinity K+ transporter 5
24.6	KUP2	potassium transporter 2
12.2	KUP6	K+ uptake permease 6
6.4	KUP6	K+ uptake permease 6
8.1	KUP6	K+ uptake permease 6
7.7	KUP6	K+ uptake permease 6
7.2	KUP8	Potassium transporter family protein
1.7	KUP11	K+ uptake permease 11
-1.5	KUP12	Potassium transporter family protein
-3.4	AKT2/3	potassium transport 2/3
-3.4	AKT2/3	potassium transport 2/3
-1.8	KEA2	K+ efflux antiporter 2
-2.1	KEA3	K+ efflux antiporter 3
-3.0	KEA3	K+ efflux antiporter 3
-2.3	KEA3	K+ efflux antiporter 3
-3.0	KEA3	K+ efflux antiporter 3
-7.2	HKT1	high-affinity K+ transporter 1
4.7	NHX1	Na+/H+ exchanger 1
2.3	SOS1	sodium proton exchanger, putative (NHX7) (SOS1)
1.7	SOS1	sodium proton exchanger, putative (NHX7) (SOS1)
2.2	ALMT13	aluminum activated malate transporter family protein
-4.6	ALMT9	aluminum-activated malate transporter 9
-2.1	SLAC1	C4-dicarboxylate transporter/malic acid transport protein
-3.0	PMT4	Major facilitator superfamily protein
-4.3	PMT5	polyol/monosaccharide transporter 5
-4.7	PMT5	polyol/monosaccharide transporter 5
24.8	STP13	Major facilitator superfamily protein
-3.9	STP5	Major facilitator superfamily protein
2.7	SUT4	sucrose transporter 4
-2.8	SUT4	sucrose transporter 4
-3.3	SWEET17	Nodulin MtN3 family protein

(Continues)

TABLE 1 (Continued)

-5.1	STP5	Major facilitator superfamily protein
-4.2	STP7	sugar transporter protein 7
-10.8	SWEET1	Nodulin MtN3 family protein
-3.6	SWEET1	Nodulin MtN3 family protein
-3.5	SWEET1	Nodulin MtN3 family protein
-2.5	SWEET17	Nodulin MtN3 family protein
-2.5	SWEET17	Nodulin MtN3 family protein
2.1	SWEET2	Nodulin MtN3 family protein
-12.7	SWEET3	Nodulin MtN3 family protein
-4.4	NAXT1	nitrate excretion transporter1
-5.9	NPF2.5	Major facilitator superfamily protein
-11.7	NRT1.2	nitrate transporter 1:2, ABA-transporter
-9.0	NRT1.1	nitrate transporter 1.1
-30.1	NRT1.1	nitrate transporter 1.1
-42.3	NRT1.1	nitrate transporter 1.1
5.4	NRT1.4	Major facilitator superfamily protein
3.8	NRT1.5	nitrate transporter 1.5, K+ loading into the xylem
-5.6	NRT1.5	nitrate transporter 1.5, K+ loading into the xylem
-2.3	NRT1.7	nitrate transporter 1.7
-2.8	NRT1.7	nitrate transporter 1.7
-2.2	NRT1.8	nitrate transporter 1.8
-2.5	NRT1.9	Major facilitator superfamily protein
-13.6	NRT2.4	nitrate transporter 2.4
-11.6	NRT2.5	nitrate transporter2.5
-2.0	SWEET17	Nodulin MtN3 family protein
-4.1	SWEET3	Nodulin MtN3 family protein
14.1	NRT1.2	nitrate transporter 1:2, ABA transporter
6.3	NRT1.3	Major facilitator superfamily protein
21.5	NRT1.4	Major facilitator superfamily protein
109.1	NRT1.5	nitrate transporter 1.5
2.8	NRT1.5	nitrate transporter 1.5
6.4	NRT1.6	nitrate transporter 1.6
2.9	NRT1.7	nitrate transporter 1.7
-9.0	NRT1.7	nitrate transporter 1.7
9.0	NRT1.7	nitrate transporter 1.7
3.6	NRT2.5	nitrate transporter2.5

Note: Both tissues apparently reduce Na^+-uptake via HKT1-channels and induce sodium efflux by SOS1, whereas genes encoding possible Cl^- exporters are preferentially induced in roots. The expression of genes encoding transporters for K^+ uptake is reduced in roots but induced in leaves. Leaves might also minimize K^+ loss by downregulation of genes encoding potassium exporters. Leaves and roots thus seem to minimize sugar transport. Transporter transcript colors: K^+ (red), Na^+ (green), Cl^- (magenta), sugar (blue), further transporters that might be permeable for chloride (black); columns salt root and salt shoot represent differentially expressed genes (fold changes) upon salt treatment. Detailed information can be found in Table S1.

part (P1), the middle part (P2), and the base (P3) of the youngest fully expanded leaf (Figure 1c). For each sample, Na^+ and K^+ concentration and transcripts of related transporters were quantified. Under control conditions, Na^+ was low in all root segments (<11 mg g DW^{-1}) (Figure 2a). Salt treatment led to a gradual increase in Na^+ from the upper root segment (17 mg g DW^{-1}) to the root apex (69 mg g DW^{-1}). Generally, ions are taken up via basipetal root segments due to a lower extent of suberinization than in the apex. In line with the Na^+ gradient in date palm root segments (Figure 2a), the expression of the *P. dactylifera* (Pd) SOS1, an ortholog of AtSOS1, *the Arabidopsis* plasma membrane localized Na^+/proton (H^+) antiporter of the NHX (Na^+/H^+ exchanger)-family, was strongly induced in the three basipetal root segments with the high Na^+ load but not in the upper segment with low Na^+ (Figure 2c). In *Arabidopsis*, the salt overly sensitive (SOS) pathway is a well-known mechanism for controlling cytosolic Na^+ concentration (Böhm et al., 2018; Shi et al., 2000, 2003). Thus, a high abundance of SOS1 in the root tips suggests a link between SOS1 abundance and Na^+ exclusion from root cells (Apse et al., 1999). However, this could not entirely prevent increasing Na^+ concentrations in the basipetal root tissue. However, foliar Na^+ concentration (<0.5 mg g DW^{-1}; Figure 2b) and foliar *PdSOS1* expression (Figure 2d) remained uncritical, that is, low, after salt exposure. The lower Na^+ concentrations in the root apex than in the tip (Figure 2a), together with the marginally increase of foliar Na^+ in response to the salt exposure, indicate that date palm reduces net Na^+ uptake and retains Na^+ from entering the shoot, respectively. Transcript levels of *PdNHX1*, an ortholog

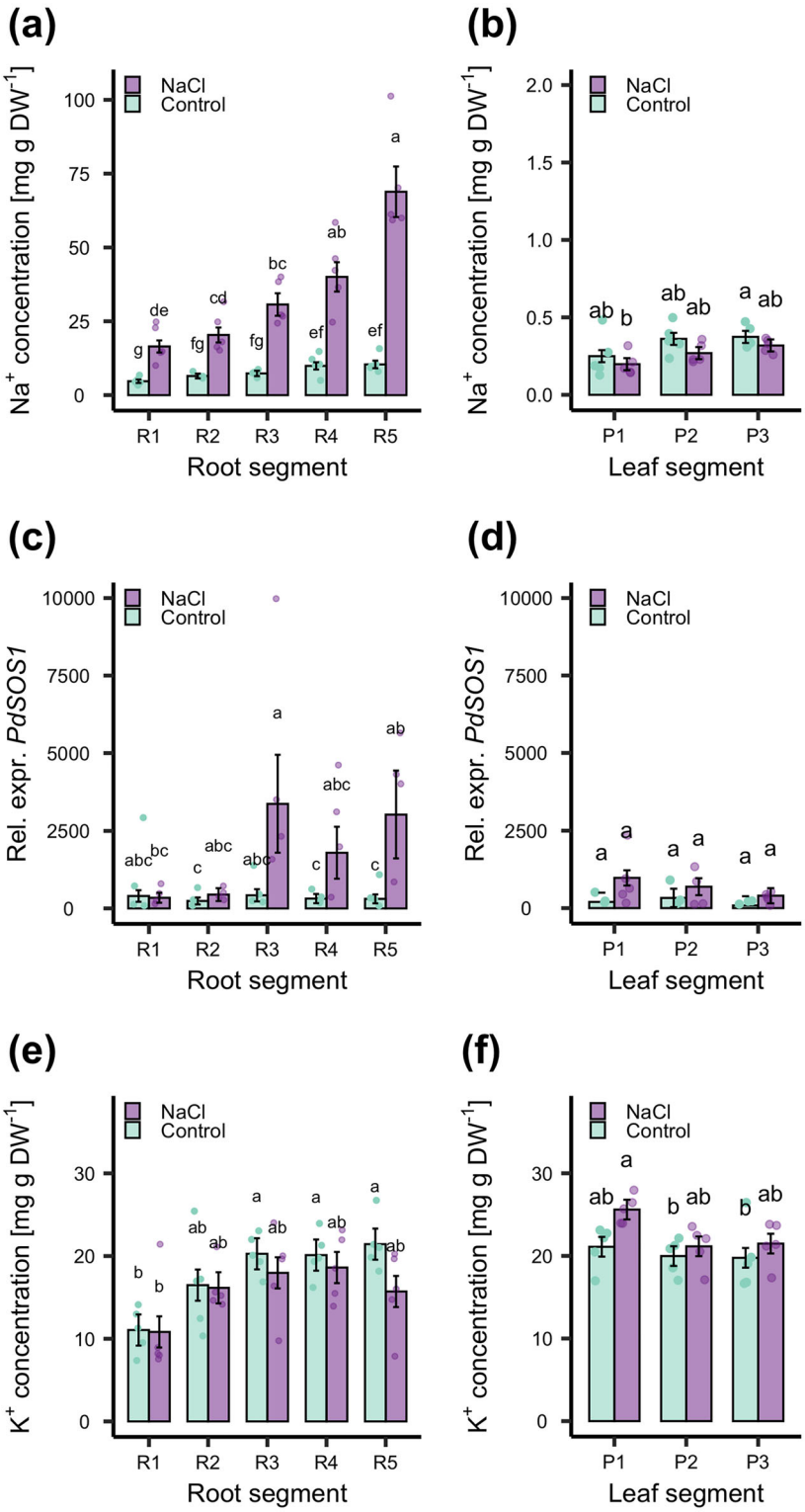

FIGURE 2 *Phoenix dactylifera* (Pd) cv. Khalas leaves and roots after 6 weeks of 600 mM NaCl treatment: (a) Sodium accumulates in root tips but not at the root/shoot transition, (b) sodium concentrations of pinnae are not affected by salt treatment, (c) elevated PdSOS1 expression in roots prevents sodium ions from reaching the leaves, transcript number is highest in root tips, (d) PdSOS1 expression in leaves does not change upon salt stress, (e and f) potassium concentrations of leaves and roots are not affected by salt treatment. Points shown represent raw data; ion measurements $n = 5$, transcript measurements $n = 3–5$; mean ± SE; Tukey's, $p \leq 0.05$; leaf *SOS1* Dunnett's T3, $p \leq 0.05$; different letters indicate significant differences of comparisons between treatments and segments.

of the vacuolar Na^+ uptake transporter (Apse et al., 1999), were not affected by salt stress in roots (Figure S1), pointing that date palms rather exclude Na^+ via SOS1 than compartmentalizing it in root vacuoles. Moreover, salt treatment did not reduce K^+ concentrations in roots or leaves (Figure 2e,f) illustrating that date palm, in addition to reducing net Na^+ uptake, is able to maintain cellular K^+ concentration and prevent displacement of K^+ by Na^+ under salt stress.

Based on these results, we performed a follow-up experiment to gain deeper insight into the salt-induced modification of the transportome and other stress protective processes. For this, date palms were cultivated in a phytotron under

desertlike climatic conditions and exposed to 600 mM NaCl over 4 weeks. In addition to analyzing the transcriptome from leaves and roots, we captured proteomic and metabolomic data as well as ion and element concentrations.

3.2 | Date palms maintain growth and prevent Cl^- and Na^+ accumulation in leaves under salinity

Consistent with our previous observations in the greenhouse (Figure 1b), salt treatment had little effect on the growth of date palm in the phytotron experiment. Shoot biomass was reduced by only one third, whereas that of roots remained unaffected after 28 days of treatment with 600 mM NaCl (Figure 3a,b). Along with the exposure to NaCl, Na^+ concentration increased in the roots, reaching 7 and 17 mg Na g^{-1} DW after 7 and 28 days, respectively (Figure 3c). However, in comparison to the greenhouse experiment, more Na^+ was transferred to the leaves. This might be attributed to the fact that plants were grown under higher light intensity in the phytotron. The more intense the light, the higher the transpiration rate and Na^+ uptake (Müller et al., 2017), as Na^+ is taken up by transpiration-driven mass flow (Yadav et al., 1996). Indeed, both experiments showed that both Na^+ and Cl^- transport from root to leaves were restricted (Figures 2a,b and 3c,d), as also observed in previous studies (Al-Bahrany & Al-Khayri, 2012; Alhammadi & Edward, 2009). Root K^+ concentration remained unchanged under NaCl stress, whereas that in the leaves even increased by 25% (Figure 3c,d). These data reveal that salt-stressed date palm Khalas is able to keep Na^+ and Cl^- concentrations low in photosynthetically active tissues while increasing leaf K^+, which helps cells to avoid a drastic decrease of the K^+:Na^+ ratio (Figure 3e,f). Concentrations of other elements (P, S, Ca, Mg, Fe, Cu, Mn, Ni, and Zn) in roots and leaves were only moderately affected by the salt treatment (Figure S2).

3.3 | Na^+, Cl^-, and K^+ transport systems are targets of root- and leaf-specific transcriptional regulation

3.3.1 | Transport of Na^+

In the greenhouse experiment, we could clearly observe a steep gradient of SOS1 expression from the root tip, where most of the ion uptake takes place, to the root base (Figure 2c). In contrast, we sampled the entire root in the phytotron experiment, that is, material from tip and base was mixed. Thus, the transcriptional gradient was masked, although very likely present. Accordingly, upon salt exposure, SOS1 transcripts appeared only slightly upregulated in the entire root samples (Table 1, Table S1c). Based on our previous results from the greenhouse experiment, we can, however, conclude that also in the phytotron experiment, SOS1 has an essential function in Na^+ exclusion from the date palm roots. Moreover, transcriptome analysis also revealed differential regulation of Na^+ permeable ion channels of the HKT family (Uozumi et al., 2000; Waters et al., 2013; Zhang et al., 2010). The downregulation of these Na^+-uptake systems was pronounced in roots (Table 1, Table S1c), where three HKT1-orthologs appeared 9- to 20-fold downregulated. In addition, two of the vacuolar NHX transporters were slightly upregulated in roots, suggesting that root cells may also compartmentalize some Na^+ in their vacuoles. Nevertheless, the exclusion of Na^+ from the root cell seems to be more efficient than depositing Na^+ via NHX in the vacuoles. These would quickly exceed their storage capacity under high salt loads as observed, for example, in the salt-sensitive gray poplar within 7–14 days of 75 mM NaCl treatment (Escalante et al., 2009).

In the leaves, only one HKT1-type transporter was downregulated, reflecting a lower requirement for prevention of Na^+ uptake by leaf cells than root cells. One NHX and two SOS1 transporters were upregulated in leaves. This indicates a viable strategy for salt tolerance: first, transferring as little Na^+ as possible to the shoot and, second, keeping Na^+ out of the cytosol of photosynthetically active leaf cells. In accordance, the transcription levels of SOS1 and the two NHX were considerably lower in the leaves than in the root.

3.3.2 | Transport of Cl^-

The anion Cl^- counterbalances Na^+ and K^+ contents (Flowers et al., 2015); however, the knowledge of Cl^- selective transporters involved in salt tolerance is yet rudimentary. No change in Cl^- concentration was found in leaves (Figure 3d), whereas Cl^- concentration in roots increased following exposure to NaCl (Figure 3c). Three out of four orthologs of the Cl^- release channels SLAH1/4 and SLAH3 were upregulated in roots in response to NaCl exposure (Table 1, Table S1c). SLAH3 is involved in the transfer of Cl^- to the leaves (Cubero-Font et al., 2016). As roots accumulated Cl^- (Figure 3c), it was not only unexpected that the Cl^- release channels were upregulated but also that NPF2.5 and NAXT1 were downregulated, which are supposed to be responsible for chloride release to the soil (reviewed by Teakle & Tyerman, 2010). However, considering that the Cl^- concentration in roots was only doubled, whereas that of Na^+ increased much more under salt stress (Figure 3c), the uptake of Cl^- into the roots may be blocked more effectively than that of Na^+, making Cl^- efflux less necessary. Recently, an ortholog of the *Arabidopsis* nitrate transporter NRT1.1 (NPF6.3) has been identified as a Cl^- uptake system in roots of *Medicago truncatula* (Xiao et al., 2021). A total of 11 of 13 date palm

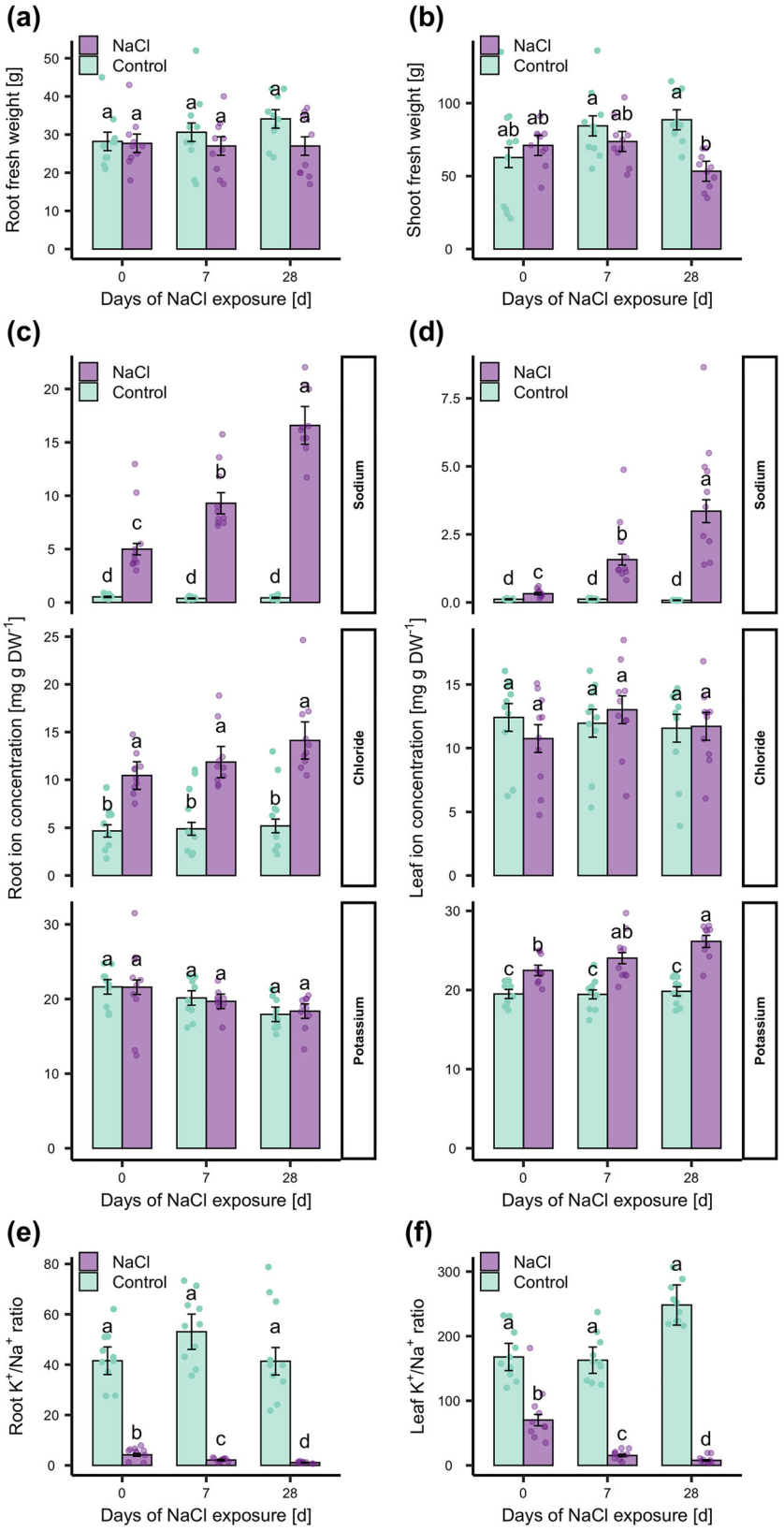

FIGURE 3 *Phoenix dactylifera* cv. Khalas biomass and elemental composition of roots and leaves after 600 mM NaCl treatment: (a) The roots show no growth depression, whereas (b) the shoot has lower biomass following 28 days salt treatment, (c) sodium and chloride accumulate in roots but potassium is not affected, (d) sodium concentrations in leaves slightly increased over time, whereas chloride and potassium concentrations were not affected, (e and f) potassium to sodium ratio in roots and leaves decreases in response to salt treatment. Points shown represent raw data; $n = 10$, mean ± SE; Tukey's, $p \leq 0.05$; different letters indicate significant differences of comparisons between treatments and days of exposure.

NRT orthologs were found to be downregulated by salinity in roots (Table 1, Table S1c). A contrasting picture was seen in the leaves, where Cl^- did not accumulate (Figure 3d). Here, 9 of 10 NRTs were induced up to 110-fold, and only one was downregulated (Table 1, Table S1d). Elemental analyses clearly showed that the transfer of excessive amounts of Cl^- from root to leaf was effectively avoided (Figure 3c,d). Thus, there must be mechanisms that attenuate the allocation

of Cl^- to the shoot to keep Cl^- away from young leaves. The transcriptome analysis does not provide a clear picture in this regard. This might be attributable to the fact that not all proteins that facilitate Cl^- transport are yet discovered or properly annotated.

3.3.3 | Transport of K^+

Plants that suffer under Na^+ toxicity usually show a decline in the intracellular concentration of K^+, whereas that of Na^+ simultaneously increases. This results a decrease in the cytosolic K^+:Na^+ ratio. As K^+ homeostasis is crucial for the activities of cytosolic enzymes (Cuin & Shabala, 2006), avoiding narrowing of the K^+:Na^+ ratio is a key trait of salt tolerant species (Escalante et al., 2009). Our transcriptomic study revealed effects on a variety of K^+ transporters of which, however, many cannot discriminate between K^+ and Na^+ when Na^+ is present at high concentrations (Blumwald et al., 2000). For this reason, the unambiguous assignment of the transport activity to either K^+ or Na^+ is not possible.

In roots, 15 out of 18 genes relevant to K^+-uptake were downregulated. Among them were four genes encoding HAK5 type high affinity K^+ transporters and seven genes encoding K^+-transporter of the KUP family (Table 1, Table S1c,e). Date palm was able to maintain the root K^+ concentration under salt stress (Figure 3c,d). The downregulation of K^+-uptake systems might be an effective strategy to avoid bypass uptake of Na^+. Strong downregulation of a gene encoding one of the SKOR-like channels in roots (Table 1) may have also contributed to maintaining K^+ homeostasis. This ortholog is likely a GORK-type K^+ release channel that removes excess K^+ from the root in *Arapidopsis* (Ivashikina et al., 2001). Moreover, the expression of a gene encoding a K^+ efflux antiporter of the KEA-type was reduced, which might prevent roots from detrimental K^+ loss (Zhao et al., 2020).

On the other hand, the upregulation of genes encoding two further members of the SKOR K^+-channel subfamily (Table 1, Table S1c,e) in roots may have contributed to the increase of the K^+ ion concentration in the leaves (Figure 3d). This is assumed because the root stele-expressed SKOR K^+ release channel is responsible for xylem loading of K^+, which is then transported acropetally to the leaves (Gaymard et al., 1998). Given that under salt stress K^+ concentration was increasing in the leaf (Figure 3d), we assume that uptake is increased, whereas the loss of K^+ from the leaves is minimized. Date palm leaves potentially counteract loss of K^+ by downregulating the expression of genes encoding five KEA-type exporters and two bidirectional AKT2/3 K^+ channels. The downregulation of these K^+ release systems could maintain K^+ homeostasis and contribute to osmotic adjustment, as reported for *Arabidopsis* (Zheng et al., 2013) and prevent detrimental K^+ efflux (Deeken et al., 2002). This is consistent with the upregulation of genes encoding four uptake channels of the shaker K^+-channel family (AKT1-, KAT1-, and KAT2-types) in leaves. Moreover, genes encoding 8 of 10 KUP/HAK-type high-affinity K^+ transporters were induced up to 25-fold in leaves under salt stress suggesting high K^+-uptake capacities (Table 1 and Table S1d,e).

The marked ability of date palm to maintain a high K^+:Na^+ ratio in leaves (Figure 3d) is based, first, on the restricted transfer of Na^+ from root to leaves. This is indicated by the induction of genes encoding the SOS1-Na^+-exporters in roots and the downregulation of genes encoding the Na^+ uptake transporter HKT1 type in aboveground tissues (Table 1 and Figure 2c). Second, it is based on increased capacities for K^+ influx into leaves. This is suggested by the upregulation of genes encoding SKOR orthologs in roots (Table 1 and Table S1c,e). As SKOR is most probably not permeable to Na^+ (Essah et al., 2003), an increase in its activity might support selective transport of K^+ to leaves. Third, the upregulation of genes encoding 12 K^+ uptake transporters (2 KAT, 2 AKT K^+ uptake channels, 1 HAK, and 7 KUP) and downregulation of genes encoding 7 K^+ release systems (5 KEA K^+ cation efflux antiporters and 2 AKT2/3 bidirectional K^+ channels) might also contribute to maintain/increase K^+ concentrations in leaves.

[Correction added on August 17, 2023, after first online publication: headings 3.3.1 and 3.3.3 showed a superscript ± (plus minus) which is updated to superscript + to indicate the cations Na^+ and K^+.]

3.4 | Roots and leaves of date palm transiently accumulate ABA following salt exposure

We analyzed the levels of the stress-related plant hormones ABA, salicylic acid (SA), and the bioactive jasmonic acid (JA) conjugate jasmonoyl isoleucine (JA-Ile) when the final salt concentration of 600 mM NaCl was reached after incremental addition of NaCl. ABA is known to accumulate in response to soil drying and salt stress (Karimi et al., 2021), leading to altered expression of thousands of genes and physiological acclimation to stress, such as the closing of stomata (Essah et al., 2003; Finkelstein & Rock, 2002; Kempa et al., 2008; Yoshida et al., 2014). This osmotically driven closure of stomata leads to decreased stomatal conductance, which in turn negatively affects CO_2 assimilation rate in date palm (Du, Ma et al., 2021; Sperling et al., 2014; Yaish et al., 2017). The latter, however, is likely being caused by ABA-mediated reduction of stomatal conductance (approx. 0.5-fold) rather than damaged photosynthetic apparatus, which might be avoided by increased non-photochemical quenching (Sperling et al., 2014). Our data show that ABA

significantly increased in response to salt exposure in both roots and leaves of date palm (Figure 4a,b). In roots, ABA concentration was increased fourfold on the day the NaCl concentration reached 600 mM (Figure 4a). ABA was still high 7 days later, suggesting that de novo root ABA biosynthesis was activated immediately at the beginning of NaCl treatment and continued at least 7 days after stress onset. However, after 28 days, ABA decreased to the level of the control. Such an ABA transient was also observed in leaves (Figure 4b), which had generally higher absolute ABA concentrations than roots. Compared to the control, leaf ABA concentration was increased about threefold on day 0 and remained elevated 4.5-fold on day 7. As in the roots, after 28 days of salt exposure, ABA again decreased to 1.5-fold that of controls. Consistently, at this time point, transcript levels of NCED (9-*cis*-epoxycarotenoid dioxygenase), the key enzyme of ABA synthesis (Malcheska et al., 2017), were similar to controls in roots and leaves (NCED 2, 3, 5, 6, and 9; Table S1b), whereas protein abundance of NCED1 was significantly decreased in leaves (−1.6-fold, Table S2). Interestingly, the transcription of some further genes involved in ABA biosynthesis remained induced although the peak in ABA concentration had already flattened (Figure 4a,b). Of these, transcripts for the last enzyme of the ABA biosynthetic pathway, the aldehyde oxidase 4 (AO4) in leaves and AO3 in roots, appeared among the seven strongest induced genes in both organs (Table S1a,b). Other genes encoding enzymes involved in ABA synthesis, such as ABA1 (in leaves and roots) and ABA3 (in leaves only), were also clearly induced. Moreover, NRT1.4-like ABA transporters were highly upregulated in the leaves (14.1-fold) and downregulated in roots (11.7-fold) (Table S1a,c). The continued upregulation of these genes might allow a rapid restoration of ABA production and could be relevant for the compartmental distribution of ABA precursors. The ABA concentration transients correlated weakly negative with the concentrations of Na^+ and Cl^- (Figure 4c–f), suggesting that date palms had already adapted to high NaCl stress after 4 weeks. Such ABA transients during long-term salt stress have been reported for *Arabidopsis* and its halophytic relative *Thellungiella* (Karimi et al., 2021). The ABA transients reported here and the previously observed slow and incomplete stomatal closure in response to petiole-fed ABA, which could be accelerated by combined petiole-supplied nitrate and ABA (Müller et al., 2017), emphasize the need for further investigation of ABA signaling and downstream acclimation responses in date palm.

3.5 | JA-Ile plays a role in in date palm leaves response to salt treatment

SA and JA are also implicated in the response of plants to salt stress (Jayakannan et al., 2015 and references therein; Riemann et al., 2015; Yu et al., 2020). Application of exogenous SA suggests that SA is involved in promoting the antioxidant system and the synthesis of osmolytes such as proline under salinity (Lee et al., 2010). However, both high SA accumulating- and SA-biosynthesis-defective *Arabidopsis* mutants are hypersensitive to salt stress, implying a dose-dependent SA regulation of salt tolerance (Borsani et al., 2001; Hao et al., 2012). In our experiment, SA concentrations were not affected by the NaCl treatment in either roots or leaves of date palm (Figure 4a,b), suggesting a minor or no role of SA in the date palm response to salt stress.

Accumulation of JA under salt stress has been observed in various species (De Domenico et al., 2019; Valenzuela et al., 2016; Zhao et al., 2014), and responses may be differentially regulated depending on spatial, temporal, and genotypic factors (Yu et al., 2020). In the roots of the halophytic date palm, the concentrations of the bioactive JA conjugate JA-Ile remained similar to controls at about 10 ng g DW^{-1} over the experimental period (Figure 4a), although seven of the eight differentially regulated genes encoding enzymes involved in JA and JA-Ile biosynthesis and metabolism were downregulated (Table S1b). In leaves, JA-Ile concentration was similar to the control even after 7 days of exposure to 600 mM NaCl, however, after 28 days, it was increased 4.9-fold (Figure 4b). Consistent with this, 9 of 10 differentially regulated genes encoding enzymes involved in JA biosynthesis and metabolism were induced in leaves (Table S1b). The results show that the JA response to salt stress occurs predominantly in the leaves rather than the roots of date palm. Stress-related JA signaling is thought to control various aspects of plant adaptation to stress (Riemann et al., 2015). Accumulation of JA is associated with growth arrest (Valenzuela et al., 2016). However, lower JA levels might also positively affect salt tolerance (Kurotani et al., 2015), probably through JA-mediated regulation of root sodium transporters (Hazman et al., 2015) and mitigation of oxidative stress (e.g., Moons et al., 1997). Salt stress causes the production of reactive oxygen species (ROS), which, in turn, activates the JA signaling pathway (Ismail et al., 2014). Although in roots, JA-Ile (Figure 4a) and H_2O_2 (Figure 5c) were not increased, in leaves, the maximum concentration of JA-Ile (Figure 4b) coincided spatiotemporally with the accumulation of ROS (approx. 0.13-fold H_2O_2) following 28 days of salt exposure (Figure 6c), suggesting a role of JA in modulating antioxidative activity in date palm. JA signaling might be integrated to ABA signaling pathways, for example, based on the interaction between (methyl-)JA-regulated stomatal closure and ABA-regulated calcium signaling (Riemann et al., 2015; Wasternack & Hause, 2013), or the requirement of JA accumulation for that of ABA in *Arabidopsis* and citrus roots (de Ollas & Dodd, 2016). In the leaves of salt stressed date palm, ABA increased before JA did (Figure 4b). As with the drought stress response, an early increase in ABA is considered the initial hormonal response to salt exposure and might therefore initiate the first line of osmotic defense, whereas the

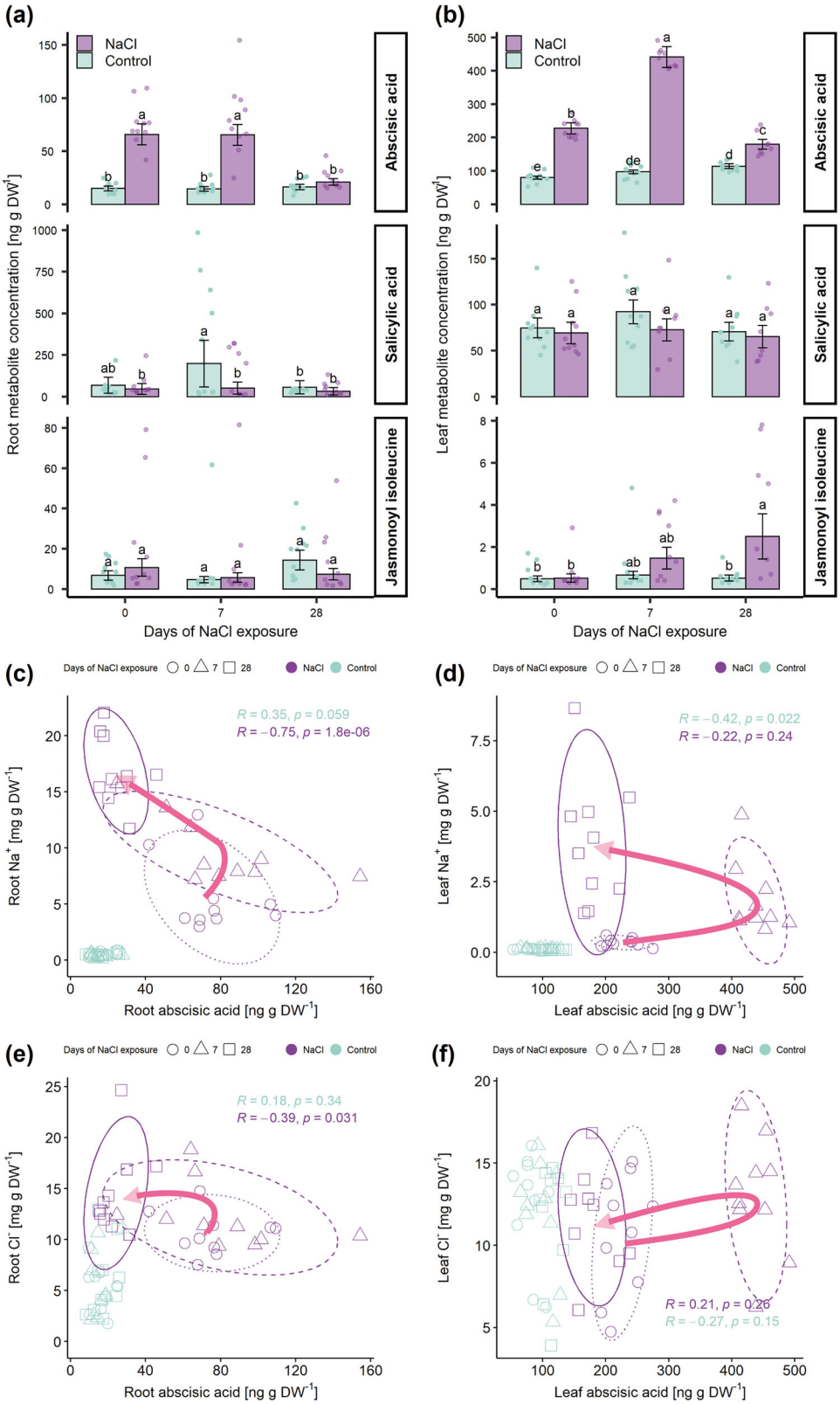

FIGURE 4 *Phoenix dactylifera* cv. Khalas transiently accumulates abscisic acid in roots and leaves after 600 mM NaCl treatment. Concentrations of abscisic- and salicylic acid, and jasmonoyl isoleucine in (a) roots and (b) leaves when the final salt concentration of 600 mM NaCl was reached after incremental addition of NaCl (day 0), and after 7 and 28 days. (c–f) Correlation of abscisic acid with sodium and chloride concentrations in root and leaves. Points shown represent raw data; $n = 8$–10, mean ± SE; Tukey's, $p \leq 0.05$; different letters indicate significant differences of comparisons between treatments and days of exposure. Arrows annotate temporal progressions via connecting centers of ellipses (level = 0.75) representing individual harvest time points.

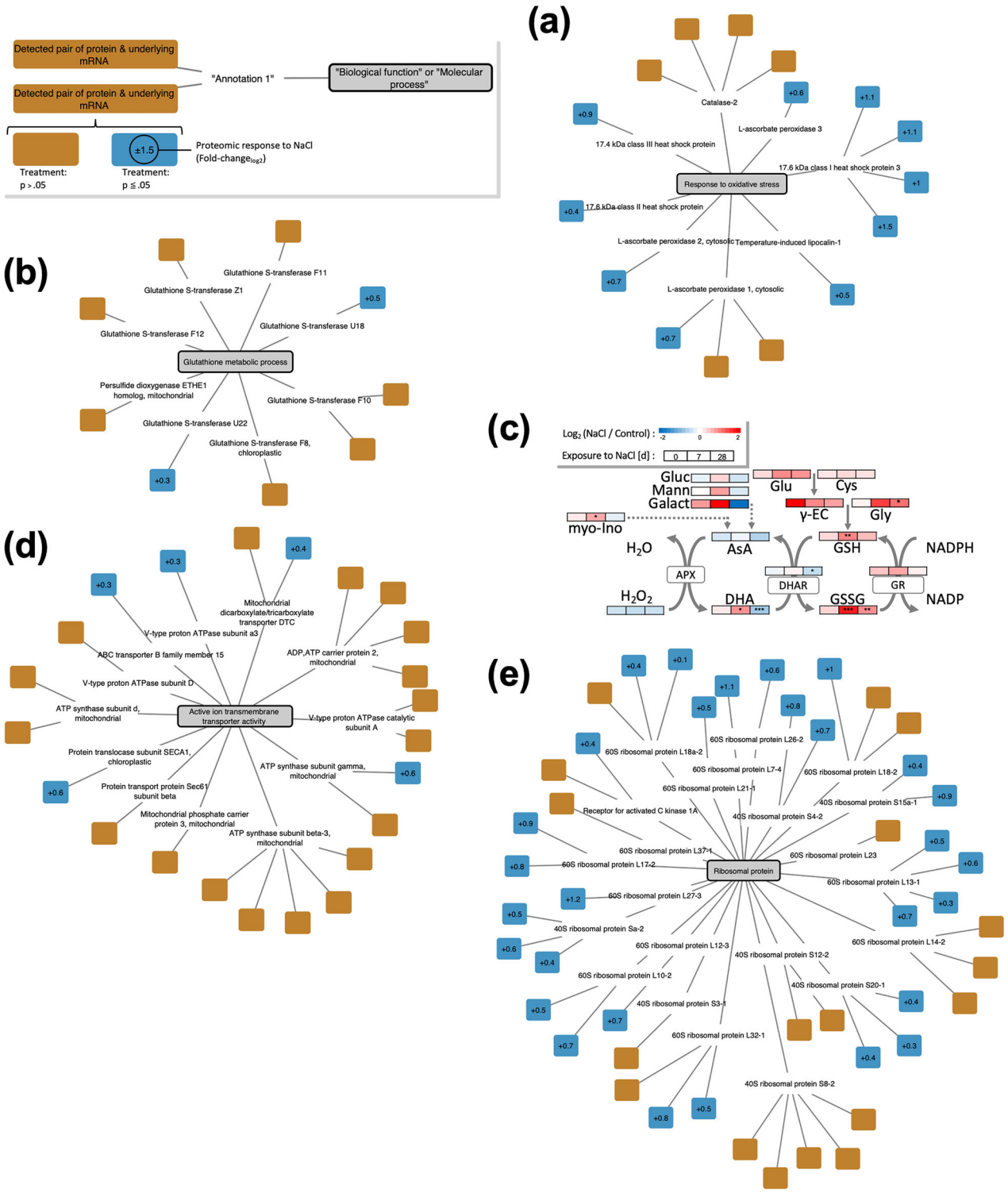

FIGURE 5 Changes in gene expression and antioxidant activity in *Phoenix dactylifera* cv. Khalas roots after treatment with 600 mM NaCl. (a and b, d and e) Networks based on combined transcriptomic and proteomic data reveal strong responses of roots to NaCl. Transcriptomic data were integrated in proteomic data, and salt-responsive proteins and underlying mRNA were identified via filtering for shared and overrepresented gene ontology (GO) terms. GO terms with respect to two domains: "Molecular Function" and "Biological Process" are shown in network hubs. Node labels show individual gene annotation. Each of the rectangular-shaped boxes in the outer layer represents a pair of protein and its underlying mRNA that are annotated to the respective gene. Blue box, salt stress-effect ($n = 4$; $p \leq 0.05$), which could be either an up- or a downregulation; brown box, no salt stress-effect. (c) Response of metabolites and enzymes assigned to total ascorbate-glutathione (GSH) cycle to salt treatment. APX, ascorbate peroxidase activity; AsA, reduced ascorbate; Cys, cysteine; DHA, dehydroascorbate; DHAR, dehydroascorbic acid reductase activity; Galac, galactose; Glu, glutamic acid; Gluc, glucose; Gly, glycine; GR, glutathione reductase activity; GSSG, glutathione disulfide; Mann, mannose; myoino, myoinositol; γ-EC, γ-glutamylcystein ($n = 5$; *t*-test; $^{*}p \leq 0.05$; $^{**}p \leq 0.01$; $^{***}p \leq 0.001$).

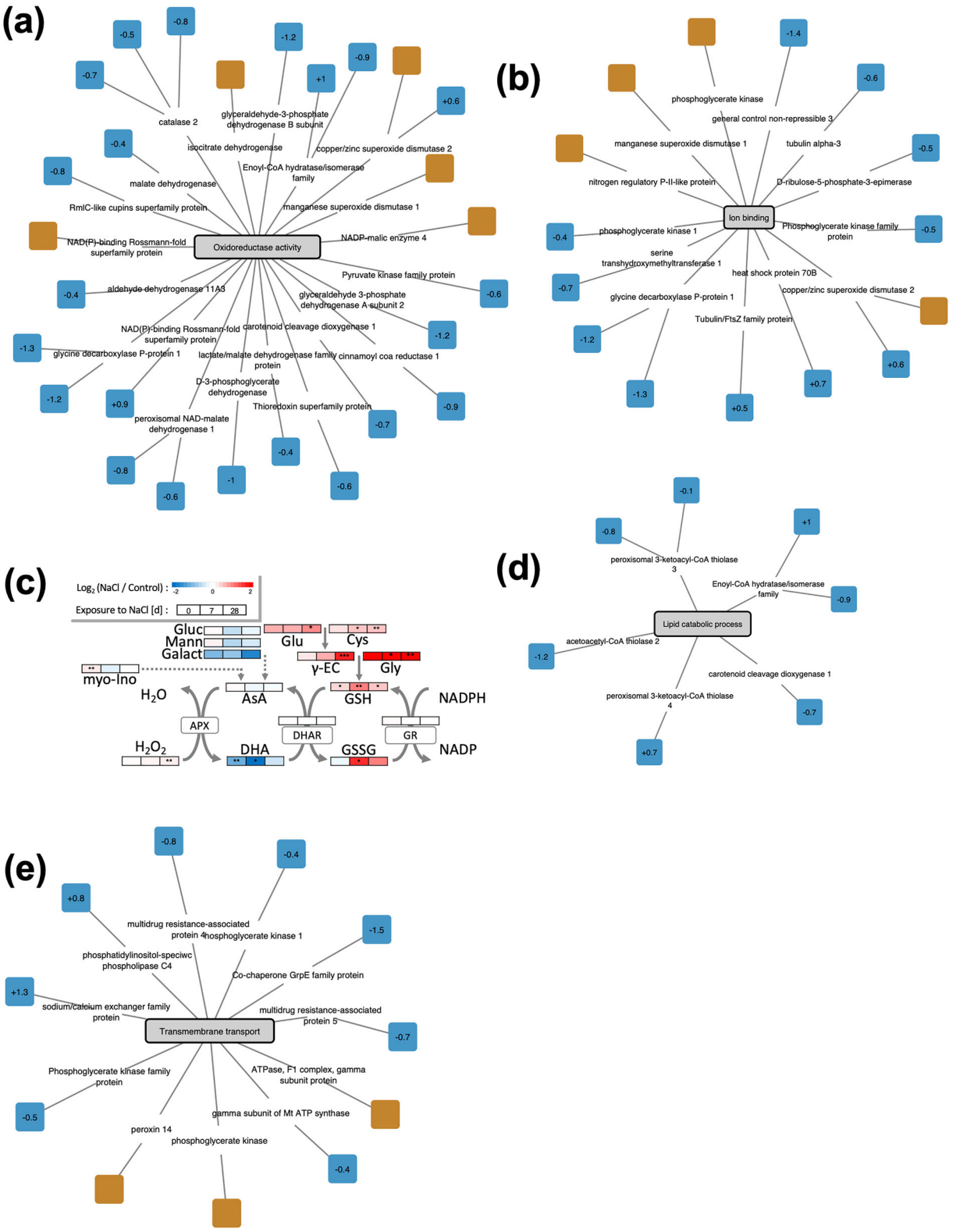

FIGURE 6 Changes in gene expression and antioxidant activity in *Phoenix dactylifera* cv. Khalas leaves after treatment with 600 mM NaCl. (a and b, d and e) Networks based on combined transcriptomic and proteomic data illustrate strong responses of leaf metabolism to NaCl treatment. (c) Response of ascorbate-glutathione cycle to NaCl treatment. Network layout, color and shape code, and abbreviations are as in Figure 4.

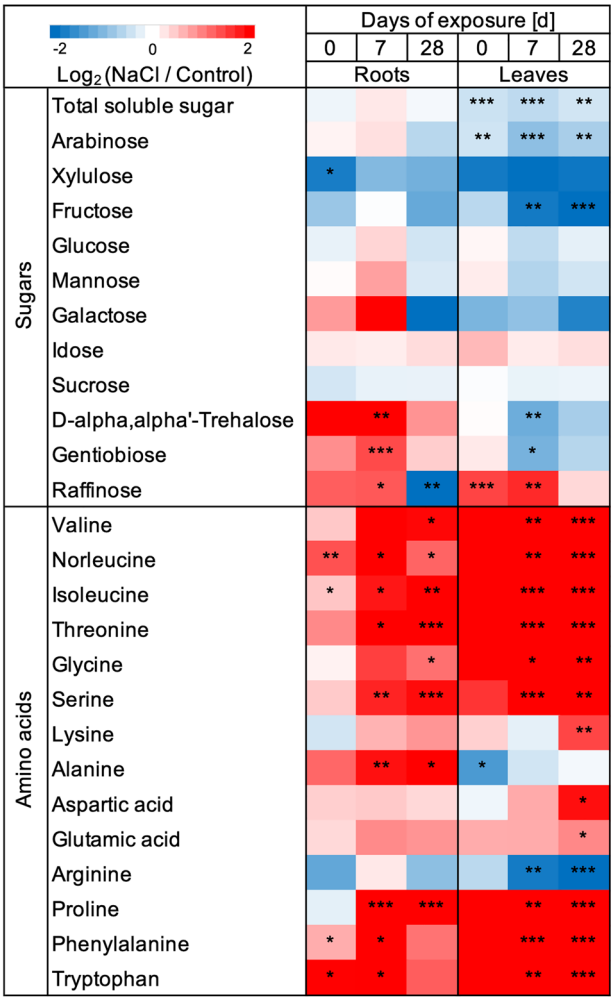

FIGURE 7 Amino acids accumulate in roots and leaves of *Phoenix dactylifera* cv. Khalas after treatment with 600 mM NaCl. Metabolic response of leaves and roots following NaCl treatment. Color scales were generated according to log2 transformed ratios between the means of salt treatment and control at 0, 8, and 28 days, respectively. Red color indicates increased abundance in salt treated plants compared to controls, and blue indicates decreased abundance upon salt treatment. Significant differences between NaCl treatment and control are indicated by asterisks ($n = 5$; t-test; $^{*}p \leq 0.05$; $^{**}p \leq 0.01$; $^{***}p \leq 0.001$; full data set provided in Figure S3).

JA-ABA interplay and a possible transition to a JA-dominated phase might allow fine-tuning of date palm's acclimation in a later period of salt stress with respect to ROS homeostasis.

3.6 | The radical detoxification machinery is booted in salt-stressed date palm

In addition to the transcriptomic data, we analyzed the abundance of enzymes involved in the salt stress response. The proteomic data (Table S2) were integrated with the transcriptomic data by identifying common and overrepresented GO features significantly regulated by the salt treatment. This approach allowed the identification of codirected changes occurring at both the transcript and protein level. Combined with the metabolic changes identified, this innovative data evaluation, visualized as networks, reveals stark information on the physiological acclimation of date palm to salt stress. Overall, this calculation provides useful insights that may not be identified from the individual analysis of transcript or protein changes alone, and it identified a high level of coverage between the regulation of transcripts and proteins. In contrast, comparative "omics"-analyses usually fail or find only weak correlations (Haider & Pal, 2013; Nie et al., 2007).

In date palm roots, 12 proteins and their underlying mRNAs with annotation to biological processes "response to oxidative stress" (GO:0006979) and "glutathione metabolic process" (GO:0006749) were upregulated (Figure 5a,b). Among them were ascorbate peroxidases (AT3G09640, AT1G07890, and AT4G35000) and GSH S-transferases (AT1G10360, AT1G78340). This is consistent with the observed response of ascorbate- GSH metabolism in roots, which was characterized by increased GSH pools but no accumulation of detrimental H_2O_2 (Figure 5c). This indicates that the adjustment of antioxidative machinery was sufficient to compensate enhanced ROS production resulting from NaCl exposure as also observed under ozone exposure (Du et al., 2018) or heat or moderate drought treatment (Arab et al., 2016). In leaves, genes related to the terms "oxidoreductase activity" (GO:0022853) and "ion binding" (GO:0043167) were both up- and downregulated in response to salt stress (Figure 6a,b). This response was based on six matches associated with the metabolism of oxygen radicals such as catalases (AT4G35090) and superoxide dismutases (AT2G28190), indicating a boost of the antioxidative machinery in response to NaCl stress. This was also reflected in constantly increased GSH pools, as observed previously under salinity (Al-Kharusi et al., 2019a). However, after 28 days of salt exposure, H_2O_2 was slightly increased (approx. 0.13-fold; Figure 6c), suggesting a slight overload of the antioxidant capacity (Goh et al., 2012). The combined results of changes in abundances of metabolites, proteins, and their underlying transcripts relevant to radical detoxification indicate that date palm increases ROS scavenging efficiency in response to NaCl stress as also observed in response to heat and drought (Arab et al., 2016; Du et al., 2021; Ghirardo et al., 2021) and ozone exposure (Du et al., 2018).

3.7 | Energy provision from catabolism and ribosome heterogeneity under salt stress

To survive extreme salinity, plants need to acclimate, which is generally an energy-consuming process (Fricke, 2020; Munns et al., 2020; Sanders, 2020). Our data raise the question as

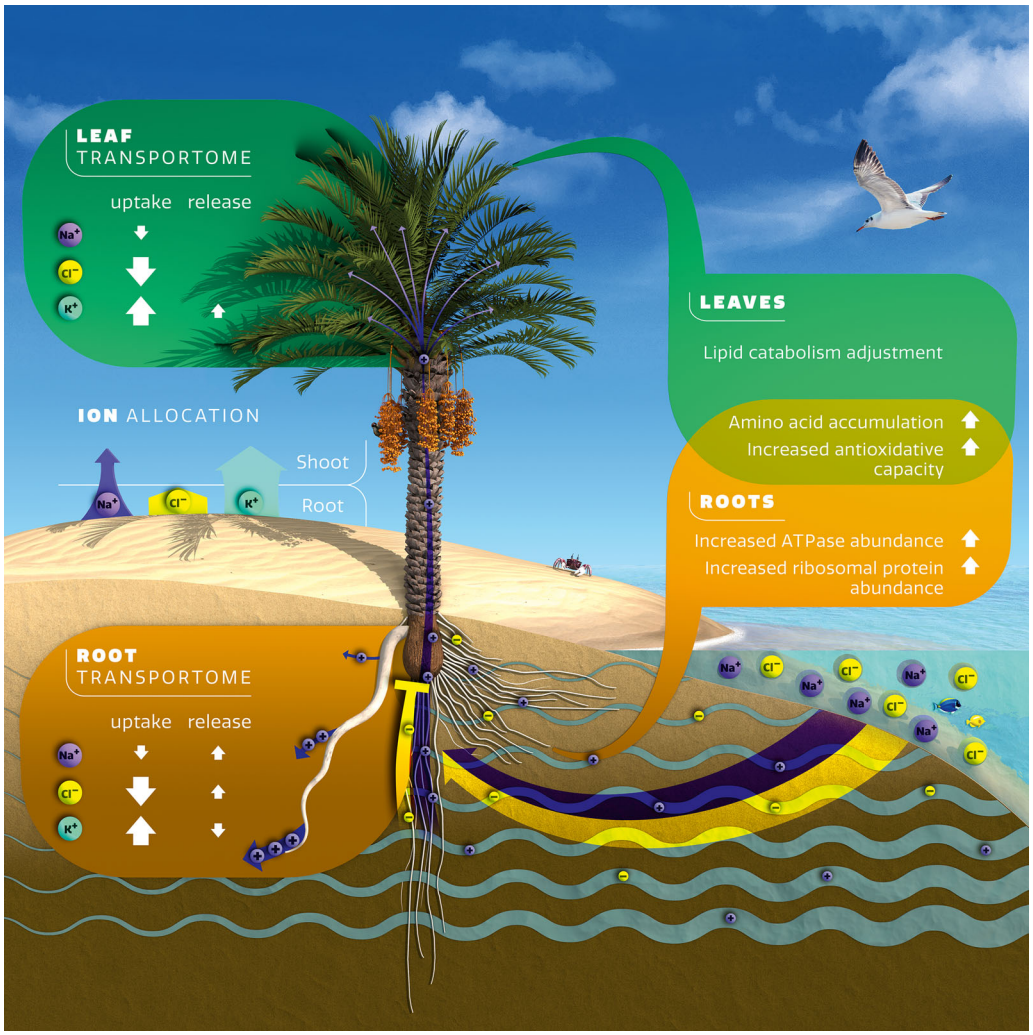

FIGURE 8 Illustration highlighting the most important findings of this study. Date palm grown in saline water restricts transport of both Na^+ and Cl^- to the shoot. Increased potassium accumulation in leaves avoids a drop in the potassium to Na^+-ratio.

to whether energy for adaptation (i.e., active ion transport, ROS detoxification, and osmotic adjustment) is derived from processes such as photosynthesis or degradation of energy-rich metabolites. The latter is vaguely suggested because proteins and the expression of underlying genes involved in energy provision from lipid degradation (GO:0016042) and the biological process "beta-oxidation of fatty acids" (GO:0006635) were overrepresented in the changes observed in date palm leaves following 28 days of salt exposure (Figure 6d and Table S2). Corroborating previous findings (Yaish et al., 2017), ATPases, which are required to sustain H^+-gradients and ATP production during oxidative phosphorylation, were constitutively strongly expressed or even upregulated in the roots of salt-stressed plants (Figure 5d). ATP is not only required for energizing salt ion exclusion but is also essential for protein synthesis, folding, and stabilization to mitigate the effects of elevated Na^+ concentrations on enzyme activities (Munns et al., 2006). In this sense, it is intriguing that proteins and genes annotated to the GO term "ribosomal protein" (GO:0003735) were highly upregulated in date palm roots after NaCl treatment (Figure 5e). K^+ is considered essential for protein biosynthesis (Kronzucker et al., 2013) and might be hampered by low K^+:Na^+ ratio under salt stress (Flowers et al., 2015). The K^+:Na^+ ratio in date palm roots decreased in response to salt exposure (Figure 3e). In line with the hypothesized relevance for plant fitness (Martinez-Seidel et al., 2020), the adaptation of the ribosome-associated proteome might be an important feature for stabilizing protein biosynthesis in the context of declining K^+:Na^+ ratio.

3.8 | Date palm accumulates amino acids as osmo-protectants

A prevalent mechanism in plants to cope with salt stress is the accumulation of compatible solutes such as amino acids, sugars, or polyols (Slama et al., 2015). Following the NaCl treatment, a variety of amino acids accumulated in both roots and leaves (Figure 7). In particular, the accumulation

of proline represents a characteristic metabolic response to salt stress in date palm (Al-Kharusi et al., 2019a, 2019b; Yaish, 2015; Yaish & Kumar, 2015) albeit less or not pronounced in cultivars considered salt sensitive, for example, cultivar Zabat (Al-Kharusi et al., 2019a). In this study, foliar proline levels increased gradually with approx. 2.5-, 4.5-, and 5.5-fold increases after 1, 8, and 28 days of salt exposure (Table S3). Depending on the dose and duration of NaCl exposure, similar (approximately twofold) (Al-Bahrany & Al-Khayri, 2012; Yaish, 2015) or smaller increases in proline have previously been observed, for example, varying between 0.2- and 0.4-fold in the salt-tolerant cultivar Umsila (Al-Kharusi et al., 2019a, 2019b). Our transcriptomic data indicate that salt stress-related proline accumulation was mediated by combined increased proline biosynthesis and reduced proline degradation. In roots and leaves, the delta1-pyrroline-5-carboxylate synthase 1 gene (P5CS1), coding for the rate-limiting enzyme in proline biosynthesis, was induced, whereas a gene (orthologs to AT5G38710) involved in proline degradation was downregulated (Table S1). In line with previous findings (Du et al., 2021), the accumulation of sugars and polyols was not observed in either the roots or the leaves (Figure S3) and individual sugars (Figure 7), including arabinose, D-fructose, and myoinositol remained unchanged or decreased. Accordingly, 11 of 12 genes encoding sugar transporters of the sweet and STP types were downregulated in roots (Table 1, Table S1c). In leaves, 8 of 10 sugar transporters of the STP, sweet, SUT, and PMT class were downregulated (Table 1, Table S1d). Consistent with the rarely observed accumulation of sugars as part of the metabolic response to salt stress in halophytes (Slama et al., 2015), date palm accumulates primarily amino acids as osmo-protectants rather than sugars.

4 | CONCLUSION

Date palm is a useful non-model crop species for learning how to survive under extreme conditions of heat, drought, or salt stress. The data presented show that date palm is able to survive extreme concentrations of Na^+ and Cl^- in the rooting solution because it effectively exerts common salt-tolerance mechanisms: (i) it restricts root uptake and transfer of Na^+ and Cl^- into the leaves while maintaining K^+-homeostasis in the leaves (Figure 8), (ii) it enhances ROS detoxification, (iii) it accumulates free amino acids to stabilize osmotic strength, and (iv) it adjusts the translational machinery in root cells affected by reduced K^+:Na^+ ratio. Together, these mechanisms contribute to keeping stress levels low, enabling date palm to grow in seawater. Based on the observed acclimation of transcription, translation, and metabolism in date palm, this integrative multi-omics approach highlights the multigenetic nature of salt tolerance, in contrast to the assumption that ion exclusion alone is responsible for date palm's salt tolerance to high soil salinity. Studying these complex processes therefore requires integrative approaches.

AUTHOR CONTRIBUTIONS

Heike Mueller: Data curation; formal analysis; investigation; writing—original draft; writing—review & editing. **Bastian Franzisky**: Data curation; formal analysis; investigation; writing—original draft; writing—review & editing. **Maxim Messerer**: Data curation; formal analysis; investigation; writing—original draft; writing—review & editing. **Baoguo Du**: Data curation; formal analysis; investigation; writing—original draft; writing—review & editing. **Thomas Lux**: Data curation; formal analysis; investigation. **Philip White**: Data curation; formal analysis; investigation. **Sebastien Carpentier**: Data curation; formal analysis; investigation; writing—original draft; writing—review & editing. **Jana Barbro Winkler**: Data curation; formal analysis; investigation. **Joerg-Peter Schnitzler**: Conceptualization; data curation; formal analysis; investigation. **Hamed El-Serehy**: Conceptualization. **Khaled Al-Rasheid**: Conceptualization; writing—original draft; writing—review & editing. **Naif Al-Harbi**: Conceptualization. **Saleh Alfarraj**: Conceptualization. **Jörg Kudla**: Conceptualization. **Jaakko Kangasjärvi**: Conceptualization. **Michael Reichelt**: Data curation; formal analysis; investigation. **Axel Mithöfer**: Data curation; formal analysis; investigation; writing—original draft; writing—review & editing. **Klaus Mayer**: Conceptualization; writing—original draft; writing—review & editing. **Heinz Rennenberg**: Conceptualization; writing—original draft; writing—review & editing. **Peter Ache**: Conceptualization; Data curation; formal analysis; investigation; writing—original draft; writing—review & editing. **Rainer Hedrich**: Conceptualization; writing—original draft; writing—review & editing. **Christoph-Martin Geilfus**: Conceptualization; data curation; formal analysis; investigation; writing—original draft; writing—review & editing.

ACKNOWLEDGMENTS

In Memoriam Professor Philip J. White (1960–2023). P.W., H.A.E.-S., N.A.-H, K.A.S.A.-R., S.A., K.F.X.M., J.Ku., J.Ka., H.R., and R.H. were supported by grants from the King Saud University, Riyadh, Saudi Arabia. This work was supported by the German Research Foundation (German: Deutsche Forschungsgemeinschaft) research grant (471624304;GZ: GE 3111/5-1).

Open access funding enabled and organized by Projekt DEAL.

CONFLICTS OF INTEREST

The authors declare that they have no known conflicts of interest or personal relationships that could have appeared to influence the work reported in this paper.

ORCID

Bastian L. Franzisky https://orcid.org/0000-0003-2590-2118
Maxim Messerer https://orcid.org/0000-0003-0554-5045
Thomas Lux https://orcid.org/0000-0002-5543-1911
Jana Barbro Winkler https://orcid.org/0000-0002-7092-9742
Michael Reichelt https://orcid.org/0000-0002-6691-6500
Klaus F. X. Mayer https://orcid.org/0000-0001-6484-1077

REFERENCES

Al-Bahrany, A. M., & Al-Khayri, J. M. (2012). In vitro responses of date palm cell suspensions under osmotic stress induced by sodium, potassium and calcium salts at different exposure durations. *American Journal of Plant Physiology*, *7*, 120–134. https://doi.org/10.3923/ajpp.2012.120.134

Alhammadi, M. S., & Edward, G. P. (2009). Effect of salinity on growth of twelve cultivars of the United Arab Emirates date palm. *Communications in Soil Science and Plant Analysis*, *40*, 2372–2388. https://doi.org/10.1080/00103620903111293

Al-Kharusi, L., Al-Yahyai, R., & Yaish, M. W. (2019a). Antioxidant response to salinity in salt-tolerant and salt-susceptible cultivars of date palm. *Agriculture*, *9*, 8. https://doi.org/10.3390/agriculture9010008

Al-Kharusi, L., Sunkar, R., Al-Yahyai, R., & Yaish, M. W. (2019b). Comparative water relations of two contrasting date palm genotypes under salinity. *International Journal of Agronomy*, *2019*, 1–16. https://doi.org/10.1155/2019/4262013

Apse, M. P., Aharon, G. S., Snedden, W. A., & Blumwald, E. (1999). Salt tolerance conferred by overexpression of a vacuolar Na^+/H^+ antiport in *Arabidopsis*. *Science*, *285*, 1256–1258. https://doi.org/10.1126/science.285.5431.1256

Arab, L., Kreuzwieser, J., Kruse, J., Zimmer, I., Ache, P., Alfarraj, S., Al-Rasheid, K. A. S., Schnitzler, J. P., Hedrich, R., & Rennenberg, H. (2016). Acclimation to heat and drought-lessons to learn from the date palm (*Phoenix dactylifera*). *Environmental and Experimental Botany*, *125*, 20–30. https://doi.org/10.1016/j.envexpbot.2016.01.003

Bhat, N. R., Suleiman, M. K., Lekha, V. S., Al-Mulla, L., Ali, S. I., George, P., & Thomas, B. (2013). Application of biosaline agriculture strategies for sustainable plant production in Kuwait. *Journal of Agriculture and Biodiversity Research*, *2*, 33–43.

Blumwald, E., Aharon, G. S., & Apse, M. P. (2000). Sodium transport in plant cells. *Biochimica et Biophysica Acta (BBA) – Biomembranes*, *1465*, 140–151. https://doi.org/10.1016/S0005-2736(00)00135-8

Böhm, J., Messerer, M., Müller, H. M., Scholz-Starke, J., Gradogna, A., Scherzer, S., Maierhofer, T., Bazihizina, N., Zhang, H., Stigloher, C., Ache, P., Al-Rasheid, K. A. S., Mayer, K. F. X., Shabala, S., Carpaneto, A., Haberer, G., Zhu, J.-K., & Hedrich, R. (2018). Understanding the molecular basis of salt sequestration in epidermal bladder cells of *Chenopodium quinoa*. *Current Biology*, *28*, 3075–3085. e3077. https://doi.org/10.1016/j.cub.2018.08.004

Bolger, A. M., Lohse, M., & Usadel, B. (2014). Trimmomatic: A flexible trimmer for Illumina sequence data. *Bioinformatics*, *30*, 2114–2120. https://doi.org/10.1093/bioinformatics/btu170

Borsani, O., Valpuesta, V., & Botella, M. A. (2001). Evidence for a role of salicylic acid in the oxidative damage generated by NaCl and osmotic stress in *Arabidopsis* seedlings. *Plant Physiology*, *126*, 1024–1030. https://doi.org/10.1104/pp.126.3.1024

Bray, N. L., Pimentel, H., Melsted, P., & Pachter, L. (2016). Near-optimal probabilistic RNA-seq quantification. *Nature Biotechnology*, *34*, 525–527. https://doi.org/10.1038/nbt.3519

Buts, K., Michielssens, S., Hertog, M. L., Hayakawa, E., Cordewener, J., America, A. H., Nicolai, B. M., & Carpentier, S. C. (2014). Improving the identification rate of data independent label-free quantitative proteomics experiments on non-model crops: A case study on apple fruit. *Journal of Proteomics*, *105*, 31–45. https://doi.org/10.1016/j.jprot.2014.02.015

Carpentier, S. C., Witters, E., Laukens, K., Deckers, P., Swennen, R., & Panis, B. (2005). Preparation of protein extracts from recalcitrant plant tissues: An evaluation of different methods for two-dimensional gel electrophoresis analysis. *Proteomics*, *5*, 2497–2507. https://doi.org/10.1002/pmic.200401222

Chen, T. H., & Murata, N. (2002). Enhancement of tolerance of abiotic stress by metabolic engineering of betaines and other compatible solutes. *Current Opinion in Plant Biology*, *5*, 250–257. https://doi.org/10.1016/S1369-5266(02)00255-8

Cubero-Font, P., Maierhofer, T., Jaslan, J., Rosales, M. A., Espartero, J., Diaz-Rueda, P., Muller, H. M., Hurter, A. L., Al-Rasheid, K. A., Marten, I., Hedrich, R., Colmenero-Flores, J. M., & Geiger, D. (2016). Silent S-type anion channel subunit SLAH1 gates SLAH3 open for chloride root-to-shoot translocation. *Current Biology*, *26*, 2213–2220. https://doi.org/10.1016/j.cub.2016.06.045

Cuin, T. A., & Shabala, S. (2006). Potassium homeostasis in salinized plant tissues. In A. G. Volkov (Ed.), *Plant electrophysiology: Theory and methods* (pp. 287–317). Springer Berlin Heidelberg.

Davila-Lara, A., Rahman-Soad, A., Reichelt, M., & Mithofer, A. (2021). Carnivorous *Nepenthes* x *ventrata* plants use a naphthoquinone as phytoanticipin against herbivory. *PLoS One*, *16*, e0258235. https://doi.org/10.1371/journal.pone.0258235

De Domenico, S., Taurino, M., Gallo, A., Poltronieri, P., Pastor, V., Flors, V., & Santino, A. (2019). Oxylipin dynamics in *Medicago truncatula* in response to salt and wounding stresses. *Physiologia Plantarum*, *165*, 198–208. https://doi.org/10.1111/ppl.12810

Deeken, R., Geiger, D., Fromm, J., Koroleva, O., Ache, P., Langenfeld-Heyser, R., Sauer, N., May, S. T., & Hedrich, R. (2002). Loss of the AKT2/3 potassium channel affects sugar loading into the phloem of *Arabidopsis*. *Planta*, *216*, 334–344. https://doi.org/10.1007/s00425-002-0895-1

Du, B., Kreuzwieser, J., Winkler, J. B., Ghirardo, A., Schnitzler, J.-P., Ache, P., Alfarraj, S., Hedrich, R., White, P., & Rennenberg, H. (2018). Physiological responses of date palm (*Phoenix dactylifera*) seedlings to acute ozone exposure at high temperature. *Environmental Pollution*, *242*, 905–913. https://doi.org/10.1016/j.envpol.2018.07.059

Du, B., Kruse, J., Winkler, J. B., Alfarraj, S., Albasher, G., Schnitzler, J.-P., Ache, P., Hedrich, R., & Rennenberg, H. (2021). Metabolic responses of date palm (*Phoenix dactylifera* L.) leaves to drought differ in summer and winter climate. *Tree Physiology*, *41*, 1685–1700. https://doi.org/10.1093/treephys/tpab027

Du, B., Ma, Y., Yanez-Serrano, A. M., Arab, L., Fasbender, L., Alfarraj, S., Albasher, G., Hedrich, R., White, P. J., Werner, C., & Rennenberg, H. (2021). Physiological responses of date palm (*Phoenix dactylifera*) seedlings to seawater and flooding. *New Phytologist*, *229*, 3318–3329. https://doi.org/10.1111/nph.17123

Du, B., Winkler, J. B., Ache, P., White, P. J., Dannenmann, M., Alfarraj, S., Albasher, G., Schnitzler, J.-P., Hedrich, R., & Rennenberg, H. (2023). Differences of nitrogen metabolism in date palm (*Phoenix dactylifera*) seedlings subjected to water deprivation and salt exposure. *Tree Physiology*, *43*, 587–596. https://doi.org/10.1093/treephys/tpac145

Escalante-Perez, M., Lautner, S., Nehls, U., Selle, A., Teuber, M., Schnitzler, J.-P., Teichmann, T., Fayyaz, P., Hartung, W., Polle, A., Fromm, J., Hedrich, R., & Ache, P. (2009). Salt stress affects xylem differentiation of grey poplar (*Populus* x *canescens*). *Planta*, *229*, 299–309. https://doi.org/10.1007/s00425-008-0829-7

Essah, P. A., Davenport, R., & Tester, M. (2003). Sodium influx and accumulation in *Arabidopsis*. *Plant Physiology*, *133*, 307–318. https://doi.org/10.1104/pp.103.022178

Finkelstein, R. R., & Rock, C. D. (2002). Abscisic acid biosynthesis and response. *The Arabidopsis Book*, *1*, e0058.

Flowers, T. J., Munns, R., & Colmer, T. D. (2015). Sodium chloride toxicity and the cellular basis of salt tolerance in halophytes. *Annals of Botany*, *115*, 419–431. https://doi.org/10.1093/aob/mcu217

Fricke, W. (2020). Energy costs of salinity tolerance in crop plants: Night-time transpiration and growth. *New Phytologist*, *225*, 1152–1165. https://doi.org/10.1111/nph.15773

Gaymard, F., Pilot, G., Lacombe, B., Bouchez, D., Bruneau, D., Boucherez, J., Michaux-Ferriere, N., Thibaud, J. B., & Sentenac, H. (1998). Identification and disruption of a plant shaker-like outward channel involved in K^+ release into the xylem sap. *Cell*, *94*, 647–655. https://doi.org/10.1016/S0092-8674(00)81606-2

Geilfus, C.-M., & Muhling, K. H. (2012). Transient alkalinization in the leaf apoplast of *Vicia faba* L. depends on NaCl stress intensity: An *in situ* ratio imaging study. *Plant, Cell and Environment*, *35*, 578–587. https://doi.org/10.1111/j.1365-3040.2011.02437.x

Ghirardo, A., Nosenko, T., Kreuzwieser, J., Winkler, J. B., Kruse, J., Albert, A., Merl-Pham, J., Lux, T., Ache, P., Zimmer, I., Alfarraj, S., Mayer, K. F. X., Hedrich, R., Rennenberg, H., & Schnitzler, J.-P. (2021). Protein expression plasticity contributes to heat and drought tolerance of date palm. *Oecologia*, *197*, 903–919. https://doi.org/10.1007/s00442-021-04907-w

Goh, C.-H., Ko, S.-M., Koh, S., Kim, Y.-J., & Bae, H.-J. (2012). Photosynthesis and environments: Photoinhibition and repair mechanisms in plants. *Journal of Plant Biology*, *55*, 93–101. https://doi.org/10.1007/s12374-011-9195-2

Haas, B. J., Papanicolaou, A., Yassour, M., Grabherr, M., Blood, P. D., Bowden, J., Couger, M. B., Eccles, D., Li, B., Lieber, M., MacManes, M. D., Ott, M., Orvis, J., Pochet, N., Strozzi, F., Weeks, N., Westerman, R., William, T., Dewey, C. N., … Regev, A. (2013). De novo transcript sequence reconstruction from RNA-seq using the Trinity platform for reference generation and analysis. *Nature Protocols*, *8*, 1494–1512. https://doi.org/10.1038/nprot.2013.084

Haider, S., & Pal, R. (2013). Integrated analysis of transcriptomic and proteomic data. *Current Genomics*, *14*, 91–110. https://doi.org/10.2174/1389202911314020003

Hao, L., Zhao, Y., Jin, D. D., Zhang, L., Bi, X. H., Chen, H. X., Xu, Q., Ma, C. Y., & Li, G. Z. (2012). Salicylic acid-altering *Arabidopsis* mutants response to salt stress. *Plant and Soil*, *354*, 81–95. https://doi.org/10.1007/s11104-011-1046-x

Hazman, M., Hause, B., Eiche, E., Nick, P., & Riemann, M. (2015). Increased tolerance to salt stress in OPDA-deficient rice ALLENE OXIDE CYCLASE mutants is linked to an increased ROS-scavenging activity. *Journal of Experimental Botany*, *66*, 3339–3352. https://doi.org/10.1093/jxb/erv142

Ismail, A., Takeda, S., & Nick, P. (2014). Life and death under salt stress: Same players, different timing? *Journal of Experimental Botany*, *65*, 2963–2979. https://doi.org/10.1093/jxb/eru159

Ivashikina, N., Becker, D., Ache, P., Meyerhoff, O., Felle, H. H., & Hedrich, R. (2001). K^+ channel profile and electrical properties of *Arabidopsis* root hairs. *FEBS Letters*, *508*, 463–469. https://doi.org/10.1016/S0014-5793(01)03114-3

Jayakannan, M., Bose, J., Babourina, O., Rengel, Z., & Shabala, S. (2015). Salicylic acid in plant salinity stress signalling and tolerance. *Plant Growth Regulation*, *76*, 25–40. https://doi.org/10.1007/s10725-015-0028-z

Karimi, S. M., Freund, M., Wager, B. M., Knoblauch, M., Fromm, J., Muller, H., Ache, P., Krischke, M., Mueller, M. J., Muller, T., Dittrich, M., Geilfus, C.-M., Alfarhan, A. H., Hedrich, R., & Deeken, R. (2021). Under salt stress guard cells rewire ion transport and abscisic acid (ABA) signaling. *New Phytologist*, *231*, 1040–1055. https://doi.org/10.1111/nph.17376

Kaushal, S. S., Likens, G. E., Pace, M. L., Utz, R. M., Haq, S., Gorman, J., & Grese, M. (2018). Freshwater salinization syndrome on a continental scale. *Proceedings of the National Academy of Sciences of the United States of America*, *115*, E574–E583.

Kempa, S., Krasensky, J., Dal Santo, S., Kopka, J., & Jonak, C. (2008). A central role of abscisic acid in stress-regulated carbohydrate metabolism. *PLoS One*, *3*, e3935. https://doi.org/10.1371/journal.pone.0003935

Kronzucker, H. J., Coskun, D., Schulze, L. M., Wong, J. R., & Britto, D. T. (2013). Sodium as nutrient and toxicant. *Plant and Soil*, *369*, 1–23. https://doi.org/10.1007/s11104-013-1801-2

Kurotani, K., Yamanaka, K., Toda, Y., Ogawa, D., Tanaka, M., Kozawa, H., Nakamura, H., Hakata, M., Ichikawa, H., Hattori, T., & Takeda, S. (2015). Stress tolerance profiling of a collection of extant salt-tolerant rice varieties and transgenic plants overexpressing abiotic stress tolerance genes. *Plant & Cell Physiology*, *56*, 1867–1876. https://doi.org/10.1093/pcp/pcv106

Lassiter, A. (2021). Rising seas, changing salt lines, and drinking water salinization. *Current Opinion in Environmental Sustainability*, *50*, 208–214. https://doi.org/10.1016/j.cosust.2021.04.009

Lee, S., Kim, S. G., & Park, C. M. (2010). Salicylic acid promotes seed germination under high salinity by modulating antioxidant activity in *Arabidopsis*. *New Phytologist*, *188*, 626–637. https://doi.org/10.1111/j.1469-8137.2010.03378.x

Li, B., Tester, M., & Gilliham, M. (2017). Chloride on the move. *Trends in Plant Science*, *22*, 236–248. https://doi.org/10.1016/j.tplants.2016.12.004

Ma, W., Liu, Z., Beier, S., Houben, A., & Carpentier, S. (2021). Identification of rye B chromosome-associated peptides by mass spectrometry. *New Phytologist*, *230*, 2179–2185. https://doi.org/10.1111/nph.17238

Malcheska, F., Ahmad, A., Batool, S., Muller, H. M., Ludwig-Muller, J., Kreuzwieser, J., Randewig, D., Hansch, R., Mendel, R. R., Hell, R., Wirtz, M., Geiger, D., Ache, P., Hedrich, R., Herschbach, C., & Rennenberg, H. (2017). Drought enhanced xylem sap sulfate closes stomata by affecting ALMT12 and guard cell ABA synthesis. *Plant Physiology*, *174*, 798–814. https://doi.org/10.1104/pp.16.01784

Martinez-Seidel, F., Beine-Golovchuk, O., Hsieh, Y. C., & Kopka, J. (2020). Systematic review of plant ribosome heterogeneity and

specialization. *Frontiers in Plant Science*, *11*, 948. https://doi.org/10.3389/fpls.2020.00948

Moons, A., Prinsen, E., Bauw, G., & Van Montagu, M. (1997). Antagonistic effects of abscisic acid and jasmonates on salt stress-inducible transcripts in rice roots. *Plant Cell*, *9*, 2243–2259.

Müller, H. M., Schafer, N., Bauer, H., Geiger, D., Lautner, S., Fromm, J., Riederer, M., Bueno, A., Nussbaumer, T., Mayer, K., Alquraishi, S. A., Alfarhan, A. H., Neher, E., Al-Rasheid, K. A. S., Ache, P., & Hedrich, R. (2017). The desert plant *Phoenix dactylifera* closes stomata via nitrate-regulated SLAC1 anion channel. *The New Phytologist*, *216*, 150–162. https://doi.org/10.1111/nph.14672

Munns, R., Day, D. A., Fricke, W., Watt, M., Arsova, B., Barkla, B. J., Bose, J., Byrt, C. S., Chen, Z. H., Foster, K. J., Gilliham, M., Henderson, S. W., Jenkins, C. L. D., Kronzucker, H. J., Miklavcic, S. J., Plett, D., Roy, S. J., Shabala, S., Shelden, M. C., … Tyerman, S. D. (2020). Energy costs of salt tolerance in crop plants. *New Phytologist*, *225*, 1072–1090. https://doi.org/10.1111/nph.15864

Munns, R., James, R. A., Gilliham, M., Flowers, T. J., & Colmer, T. D. (2016). Tissue tolerance: An essential but elusive trait for salt-tolerant crops. *Functional Plant Biology*, *43*, 1103–1113. https://doi.org/10.1071/FP16187

Munns, R., James, R. A., & Läuchli, A. (2006). Approaches to increasing the salt tolerance of wheat and other cereals. *Journal of Experimental Botany*, *57*, 1025–1043. https://doi.org/10.1093/jxb/erj100

Munns, R., & Millar, A. H. (2023). Seven plant capacities to adapt to abiotic stress. *Journal of Experimental Botany*. https://doi.org/10.1093/jxb/erad179

Munns, R., & Tester, M. (2008). Mechanisms of salinity tolerance. *Annual Review of Plant Biology*, *59*, 651–681. https://doi.org/10.1146/annurev.arplant.59.032607.092911

Nie, L., Wu, G., Culley, D. E., Scholten, J. C. M., & Zhang, W. (2007). Integrative analysis of transcriptomic and proteomic data: Challenges, solutions and applications. *Critical Reviews in Biotechnology*, *27*, 63–75. https://doi.org/10.1080/07388550701334212

Okur, B., & Örçen, N. (2020). Soil salinization and climate change. In *Climate change and soil interactions*. (pp. 331–350). Elsevier.

Paoletti, E., Hoshika, Y., Arab, L., Martini, S., Cotrozzi, L., Weber, D., Ache, P., Neri, L., Baraldi, R., Pellegrini, E., Müller, H. M., Hedrich, R., Alfarraj, S., & Rennenberg, H. (2021). Date palm responses to a chronic, realistic ozone exposure in a FACE experiment. *Environmental Research*, *195*, 110868. https://doi.org/10.1016/j.envres.2021.110868

Patankar, H. V., Assaha, D. V. M., Al-Yahyai, R., Sunkar, R., & Yaish, M. W. (2016). Identification of reference genes for quantitative real-time PCR in date palm (*Phoenix dactylifera* L.) subjected to drought and salinity. *PLoS One*, *11*, e0166216. https://doi.org/10.1371/journal.pone.0166216

Polle, A., Chakrabarti, K., Schurmann, W., & Renneberg, H. (1990). Composition and properties of hydrogen peroxide decomposing systems in extracellular and total extracts from needles of Norway spruce (*Picea abies* L., Karst.). *Plant Physiology*, *94*, 312–319. https://doi.org/10.1104/pp.94.1.312

R Core Team. (2020). *R: A language and environment for statistical computing*. R Foundation for Statistical Computing. URL https://www.r-project.org/

Riemann, M., Dhakarey, R., Hazman, M., Miro, B., Kohli, A., & Nick, P. (2015). Exploring jasmonates in the hormonal network of drought and salinity responses. *Frontiers in Plant Science*, *6*, 1077. https://doi.org/10.3389/fpls.2015.01077

Robinson, M. D., McCarthy, D. J., & Smyth, G. K. (2010). edgeR: A bioconductor package for differential expression analysis of digital gene expression data. *Bioinformatics*, *26*, 139–140. https://doi.org/10.1093/bioinformatics/btp616

Rubio, F., Nieves-Cordones, M., Horie, T., & Shabala, S. (2020). Doing 'business as usual' comes with a cost: Evaluating energy cost of maintaining plant intracellular K^+ homeostasis under saline conditions. *New Phytologist*, *225*, 1097–1104. https://doi.org/10.1111/nph.15852

Samuilov, S., Lang, F., Djukic, M., Djunisijevic-Bojovic, D., & Rennenberg, H. (2016). Lead uptake increases drought tolerance of wild type and transgenic poplar (*Populus tremula* x *P. alba*) overexpressing gsh 1. *Environmental Pollution*, *216*, 773–785. https://doi.org/10.1016/j.envpol.2016.06.047

Sanders, D. (2020). The salinity challenge. *New Phytologist*, *225*, 1047–1048. https://doi.org/10.1111/nph.16357

Schupp, R., & Rennenberg, H. (1988). Diurnal changes in the glutathione content of spruce needles (*Picea abies* L.). *Plant Science*, *57*, 113–117. https://doi.org/10.1016/0168-9452(88)90076-3

Shannon, P., Markiel, A., Ozier, O., Baliga, N. S., Wang, J. T., Ramage, D., Amin, N., Schwikowski, B., & Ideker, T. (2003). Cytoscape: A software environment for integrated models of biomolecular interaction networks. *Genome Research*, *13*, 2498–2504. https://doi.org/10.1101/gr.1239303

Shi, H., Ishitani, M., Kim, C., & Zhu, J. K. (2000). The *Arabidopsis thaliana* salt tolerance gene SOS1 encodes a putative Na^+/H^+ antiporter. *PNAS*, *97*, 6896–6901. https://doi.org/10.1073/pnas.120170197

Shi, H., Lee, B. H., Wu, S. J., & Zhu, J. K. (2003). Overexpression of a plasma membrane Na^+/H^+ antiporter gene improves salt tolerance in *Arabidopsis thaliana*. *Nature Biotechnology*, *21*, 81–85. https://doi.org/10.1038/nbt766

Slama, I., Abdelly, C., Bouchereau, A., Flowers, T., & Savoure, A. (2015). Diversity, distribution and roles of osmoprotective compounds accumulated in halophytes under abiotic stress. *Annals of Botany*, *115*, 433–447. https://doi.org/10.1093/aob/mcu239

Soares, A. L. C., Geilfus, C.-M., & Carpentier, S. C. (2018). Genotype-specific growth and proteomic responses of maize toward salt stress. *Frontiers in Plant Science*, *9*, 661. https://doi.org/10.3389/fpls.2018.00661

Sperling, O., Lazarovitch, N., Schwartz, A., & Shapira, O. (2014). Effects of high salinity irrigation on growth, gas-exchange, and photoprotection in date palms (*Phoenix dactylifera* L., cv. Medjool). *Environmental and Experimental Botany*, *99*, 100–109. https://doi.org/10.1016/j.envexpbot.2013.10.014

Strohm, M., Jouanin, L., Kunert, K. J., Pruvost, C., Polle, A., Foyer, C. H., & Rennenberg, H. (1995). Regulation of glutathione synthesis in leaves of transgenic poplar (*Populus tremula* X *P. alba*) overexpressing glutathione synthetase. *Plant Journal*, *7*, 141–145. https://doi.org/10.1046/j.1365-313X.1995.07010141.x

Teakle, N. L., & Tyerman, S. D. (2010). Mechanisms of Cl^- transport contributing to salt tolerance. *Plant, Cell & Environment*, *33*, 566–589.

Uozumi, N., Kim, E. J., Rubio, F., Yamaguchi, T., Muto, S., Tsuboi, A., Bakker, E. P., Nakamura, T., & Schroeder, J. I. (2000). The *Arabidopsis* HKT1 gene homolog mediates inward Na^+ currents in *Xenopus*

laevis oocytes and Na^+ uptake in *Saccharomyces cerevisiae*. *Plant Physiology*, *122*, 1249–1259. https://doi.org/10.1104/pp.122.4.1249

Vadassery, J., Reichelt, M., Hause, B., Gershenzon, J., Boland, W., & Mithofer, A. (2012). CML42-mediated calcium signaling coordinates responses to *Spodoptera* herbivory and abiotic stresses in *Arabidopsis*. *Plant Physiology*, *159*, 1159–1175. https://doi.org/10.1104/pp.112.198150

Valenzuela, C. E., Acevedo-Acevedo, O., Miranda, G. S., Vergara-Barros, P., Holuigue, L., Figueroa, C. R., & Figueroa, P. M. (2016). Salt stress response triggers activation of the jasmonate signaling pathway leading to inhibition of cell elongation in *Arabidopsis* primary root. *Journal of Experimental Botany*, *67*, 4209–4220. https://doi.org/10.1093/jxb/erw202

van Wesemael, J., Hueber, Y., Kissel, E., Campos, N., Swennen, R., & Carpentier, S. (2018). Homeolog expression analysis in an allotriploid non-model crop via integration of transcriptomics and proteomics. *Scientific Reports*, *8*, 1353. https://doi.org/10.1038/s41598-018-19684-5

Velikova, V., Yordanov, I., & Edreva, A. (2000). Oxidative stress and some antioxidant systems in acid rain-treated bean plants – Protective role of exogenous polyamines. *Plant Science*, *151*, 59–66. https://doi.org/10.1016/S0168-9452(99)00197-1

Wasternack, C., & Hause, B. (2013). Jasmonates: Biosynthesis, perception, signal transduction and action in plant stress response, growth and development. An update to the 2007 review in Annals of Botany. *Annals of Botany*, *111*, 1021–1058. https://doi.org/10.1093/aob/mct067

Waters, S., Gilliham, M., & Hrmova, M. (2013). Plant high-affinity potassium (HKT) transporters involved in salinity tolerance: Structural insights to probe differences in ion selectivity. *International Journal of Molecular Sciences*, *14*, 7660–7680. https://doi.org/10.3390/ijms14047660

White, P. J., Broadley, M. R., Thompson, J. A., McNicol, J. W., Crawley, M. J., Poulton, P. R., & Johnston, A. E. (2012). Testing the distinctness of shoot ionomes of angiosperm families using the Rothamsted Park Grass Continuous Hay Experiment. *New Phytologist*, *196*, 101–109. https://doi.org/10.1111/j.1469-8137.2012.04228.x

Wickham, H. (2016). *ggplot2: Elegant graphics for data analysis*. Springer-Verlag. https://ggplot2.tidyverse.org

Xiao, Q., Chen, Y., Liu, C. W., Robson, F., Roy, S., Cheng, X., Wen, J., Mysore, K., Miller, A. J., & Murray, J. D. (2021). MtNPF6.5 mediates chloride uptake and nitrate preference in Medicago roots. *EMBO Journal*, *40*, e106847. https://doi.org/10.15252/embj.2020106847

Yadav, R., Flowers, T. J., & Yeo, A. R. (1996). The involvement of the transpirational bypass flow in sodium uptake by high- and low- sodium-transporting lines of rice developed through intravarietal selection. *Plant Cell and Environment*, *19*, 329–336. https://doi.org/10.1111/j.1365-3040.1996.tb00255.x

Yaish, M. W. (2015). Proline accumulation is a general response to abiotic stress in the date palm tree (*Phoenix dactylifera* L.). *Genetics and Molecular Research*, [Electronic Resource], *14*, 9943–9950. https://doi.org/10.4238/2015.August.19.30

Yaish, M. W., & Kumar, P. P. (2015). Salt tolerance research in date palm tree (*Phoenix dactylifera* L.), past, present, and future perspectives. *Frontiers in Plant Science*, *6*, 348. https://doi.org/10.3389/fpls.2015.00348

Yaish, M. W., Patankar, H. V., Assaha, D. V. M., Zheng, Y., Al-Yahyai, R., & Sunkar, R. (2017). Genome-wide expression profiling in leaves and roots of date palm (*Phoenix dactylifera* L.) exposed to salinity. *BMC Genomics*, [Electronic Resource], *18*, 246. https://doi.org/10.1186/s12864-017-3633-6

Yoshida, T., Mogami, J., & Yamaguchi-Shinozaki, K. (2014). ABA-dependent and ABA-independent signaling in response to osmotic stress in plants. *Current Opinion in Plant Biology*, *21*, 133–139. https://doi.org/10.1016/j.pbi.2014.07.009

Yu, Z., Duan, X., Luo, L., Dai, S., Ding, Z., & Xia, G. (2020). How plant hormones mediate salt stress responses. *Trends in Plant Science*, *25*, 1117–1130. https://doi.org/10.1016/j.tplants.2020.06.008

Zhang, J. L., Flowers, T. J., & Wang, S. M. (2010). Mechanisms of sodium uptake by roots of higher plants. *Plant and Soil*, *326*, 45–60. https://doi.org/10.1007/s11104-009-0076-0

Zhao, C., Zhang, H., Song, C. P., Zhu, J. K., & Shabala, S. (2020). Mechanisms of plant responses and adaptation to soil salinity. *The Innovation*, *1*, 100017. https://doi.org/10.1016/j.xinn.2020.100017

Zhao, Y., Dong, W., Zhang, N., Ai, X., Wang, M., Huang, Z., Xiao, L., & Xia, G. (2014). A wheat allene oxide cyclase gene enhances salinity tolerance via jasmonate signaling. *Plant Physiology*, *164*, 1068–1076. https://doi.org/10.1104/pp.113.227595

Zheng, S., Pan, T., Fan, L., & Qiu, Q. S. (2013). A novel AtKEA gene family, homolog of bacterial K^+/H^+ antiporters, plays potential roles in K^+ homeostasis and osmotic adjustment in *Arabidopsis*. *PLoS One*, *8*, e81463. https://doi.org/10.1371/journal.pone.0081463

SUPPORTING INFORMATION

Additional supporting information can be found online in the Supporting Information section at the end of this article. [Correction added on August 17, 2023, after first online publication: Supplementary files are updated.]

How to cite this article: Mueller, H. M., Franzisky, B. L., Messerer, M., Du, B., Lux, T., White, P. J., Carpentier, S. C., Winkler, J. B., Schnitzler, J.-P., El-Serehy, H. A., Al-Rasheid, K. A. S., Al-Harbi, N., Alfarraj, S., Kudla, J., Kangasjärvi, J., Reichelt, M., Mithöfer, A., Mayer, K. F. X., Rennenberg, H., … Geilfus, C.-M. (2024). Integrative multi-omics analyses of date palm (*Phoenix dactylifera*) roots and leaves reveal how the halophyte land plant copes with sea water. *The Plant Genome*, *17,* e20372. https://doi.org/10.1002/tpg2.20372